THE MINERALOGICAL MAGAZINE

AND

JOURNAL OF

THE MINERALOGICAL SOCIETY

No. 200 March, 1948 Vol. XXVIII

The occurrence of an orthorhombic high-temperature form of Ca_2SiO_4 (bredigite) in the Scawt Hill contact-zone and as a constituent of slags.

(With Plates XV and XVI.)

By C. E. Tilley, F.R.S., and H. C. G. Vincent, M.A.

Department of Mineralogy and Petrology, University of Cambridge.

[Read November 6, 1947.]

Introduction.

RECENT research on the polymorphism of calcium orthosilicate has broadened and to some extent modified the picture of the phase relations of this substance as presented in the pioneer studies of Day and Shepherd (1906) and Rankin and Wright (1915). These investigators recognized three distinct forms, α, β, and γ, related by transformation as follows: $\alpha \rightleftarrows \beta$ at 1420° C. and $\beta \rightleftarrows \gamma$ at 675° C. The high-temperature α form was described as monoclinic or triclinic and intimately twinned, the β form orthorhombic, and the low-temperature γ form as probably monoclinic. The optical properties of these α and β forms as reported are so closely similar that were it not for the twinning, regarded as diagnostic, the two forms would be distinguishable only with difficulty. This optical similarity was later found to be paralleled by a close agreement of the X-ray powder diffraction patterns of the two phases early noted by Hansen (1928) and confirmed among others by Insley (1936). These similarities led both these workers to the conclusion that the α form actually may never have been observed, the intimate twinning of the supposed α form appearing as a consequence of rapid inversion of a high-temperature form to the β form. The leucite analogy thus inferred appeared a logical interpretation of the evidence when critically examined.

Such was the position reached in studies up to 1941. At that time Bredig (1941, 1942), who had been investigating the structures of calcium phosphates and had under study a group of compounds of the general formula A_2XO_4, reviewed the evidence for the existence of the 'ternary compounds' in the system CaO–SiO_2–P_2O_5 and indicated the probability that the substance $7CaO.P_2O_5.2SiO_2$ possessed the simple crystal lattice of a group of simple compounds of the type A_2XO_4, e.g. K_2SO_4, $CaKPO_4$, the high-temperature α (hexagonal) modifications of which form extensive solid solutions with other compounds. He was led to infer, partly on evidence of X-ray powder photographs, that the 'compound' referred to was in fact a solid solution of an α-Ca_2SiO_4 (hexagonal) phase analogous to α hexagonal K_2SO_4 or glaserite $(K,Na)_2SO_4$. Similarly, Bredig (1942, 1943) claimed another 'compound' in this system $27CaO.P_2O_5.12SiO_2$, described by Schleede (1940) with a β-K_2SO_4 structure, to be in fact an orthorhombic Ca_2SiO_4 (designated as α'-Ca_2SiO_4) solid solution to which also the 'K' phase of Trömel (1943) in the same silicophosphate system and the 'compound' $K_2O.23CaO.12SiO_2$ prepared by Taylor (1941) in Portland cement studies belonged. Bredig concluded that pure Ca_2SiO_4 would be expected to possess in its various forms an α hexagonal and a β (but now designated, as noted above, α') orthorhombic structure, in addition to the usual β and γ (olivine type[1]) structures of the forms described by Day and Shepherd, and that the α' form would be expected to be stable in the temperature region between an α (high, hexagonal) field of stability and the temperature of 1420° C. when the β-Ca_2SiO_4 stability region is entered.

In 1944 Greene published his study of dicalcium silicate solid solutions, obtaining an optically positive uniaxial form of the orthosilicate (containing Na_2O and Al_2O_3 in solid solution) and showing in its X-ray powder pattern the structure of the α hexagonal A_2XO_4 group.

Still more recently Van Valkenburg and McMurdie (1947) have prepared and examined pure Ca_2SiO_4 in a high-temperature X-ray powder diffraction furnace at 1500° C. obtaining a characteristic hexagonal pattern. Bredig's prediction in this connexion has thus been amply justified.

It was in the light of these conclusions that a restudy was begun of a number of larnite assemblages of the Scawt Hill contact-zone. It had already become clear from the earlier work reported that the mineral

[1] The γ phase formerly referred to as monoclinic was shown by O'Daniel and Tscheischwili (Zeits. Krist., 1942, vol. 104, pp. 124–141) to be orthorhombic with the olivine structure. [M.A. 8–290.]

larnite with its characteristic twinning was to be referred to β-Ca_2SiO_4, which phase in view of the optical data available should be regarded as monoclinic in character. In some of the Scawt Hill assemblages rare isolated grains of a pseudo-hexagonal mineral with a low optic axial angle had long been observed but its composition had remained undetermined, though its paragenesis suggested that it was a calcium silicate. At the time of this later study a group of spiegeleisen slags containing an obvious Ca_2SiO_4 phase was under examination. This orthosilicate phase of the slag was characterized by an optic axial angle much smaller than that usually found in larnite and, though twinned, it had not the normal twin pattern of that mineral. There was reason to believe that the rare Scawt Hill mineral and the mineral of the slag were probably identical and accordingly a more detailed examination of the suite of Scawt Hill rocks was made to ascertain if more of the material could be made available for identification. Fortunately this has proved successful and a parallel examination of the natural and the slag mineral has been made. Both have proved to be orthorhombic, pseudo-hexagonal in character, the abundance of the slag phase allowing its isolation for chemical analysis. The results now set down indicate that the two minerals are in fact the predicted orthorhombic silicate structure designated as α'-Ca_2SiO_4 by Bredig, but that in the case of the slag phase a considerable amount of material in solid solution is present. It is in recognition of Bredig's important contribution to the solution of the problem of calcium orthosilicate polymorphism that it is proposed to designate the new mineral phase *bredigite*.[1]

The Scawt Hill mineral.

The new phase occurs together with spurrite, larnite, and gehlenite. Though never abundant, it is rather widely distributed in a group of rocks composed of these minerals in the form of squat orthorhombic grains showing in cross-section hexagonal outline and in vertical section barrel- or boat-shaped forms. The appearance of these crystals is indicated in pl. XV, figs. 1, 2, and 4. In the cross-sections twin structure is commonly apparent, the twinning being simple, multiple, or even cyclic. Such cross-sections show the normal emergence of an acute bisectrix and exhibit traces of cleavages, obviously prismatic, forming angles of approximately 60°. The vertical sections show parallel extinction with reference to the cleavage trace, this being slow parallel

[1] The mineral has, more recently, been observed in the limestone contact-zone of the Camas Mòr gabbro of the island of Muck, Inverness-shire.

to the acute bisectrix (γ). A good example of a cross-section showing simple twinning is seen in pl. XV, figs. 2 and 4.

The relation of the optical features to the twinning and cleavages is reproduced in the simple and cyclic twins of text-fig. 1. The optic axial plane forms an angle of approximately 60° with the trace of the composition (twin) plane and bisects the acute angle between the two cleavages of each part of the twin. The extinction in these basal sections is β:twin-plane = 30°. These optical properties are those characteristic

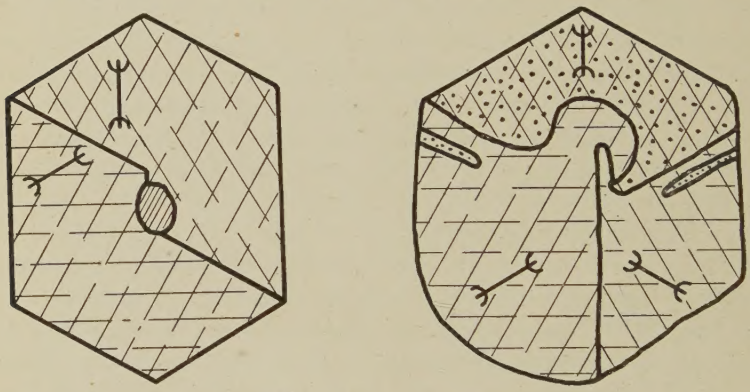

FIG. 1. Basal sections of bredigite in spurrite-larnite-rocks, showing simple and cyclic twinning. If by analogy with β-K_2SO_4 the optic axial plane is taken as (100), the prismatic cleavages at approximately 60° become (110), and the twin-plane (130). In the left-hand crystal the central inclusion is larnite cut perpendicular to the acute bisectrix (γ) with the twin striae indicated.

of an orthorhombic pseudo-hexagonal structure, reproducing in essence the features encountered in the sulphates of the alkali metals. If by analogy with β-K_2SO_4 we arbitrarily define the optic axial plane as (100), the prismatic cleavages become (110) and the twin-plane (130) (text-figs. 1 and 2).

The optical properties of the mineral may be summarized as follows: $\gamma = c$, $\alpha = b$, $\beta = a$; 2V 30°, but variable, lower values being also recorded; α 1·712, β 1·716, γ 1·725.

Grains isolated from their matrix dissolve readily in the weakest acids leaving a silica pseudomorph, give no effervescence, and yield abundant evidence of calcium. They behave in these respects like larnite itself.

In many of the sections the grains stand out from enclosing larnite or spurrite because they exhibit in patches a fibrous structure reducing their translucency under low power. Their refraction is not greatly different from larnite, and where this fibrous character is absent they

differ in section by the presence of better developed cleavage lines. The basal sections are of course distinctive. Examination of this fibrous development shows that the optical properties of the fibrous element are noticeably different from those of the normal non-fibrous part of the mineral. The fibres have in fact the optical characters of the low γ form of Ca_2SiO_4, lower refraction, negative sign, and the optic axial plane across the length of the fibre (elongation $\pm$). It is clear that such composite grains are the new phase associated with its inversion product. Occasionally the transformation may be seen complete. Normally the fibres of the γ form run parallel to the cleavage of the parent phase as seen in the vertical sections. In basal section the fibres appear as sheets or bunches for the most part oriented in the 60° prismatic cleavage directions and extinguishing with the main mineral. At first sight these sheets have the appearance of foreign material developed by exsolution, but closer examination reveals that they have the properties of γ-Ca_2SiO_4, being viewed along the direction β and so exhibiting the maximum birefringence. None of this sheet development appears in the basal sections of grains which show in vertical section no sign of the fibrous development already noted. There is clearly evidence that the inversion product is regularly oriented, for the most part, in relation to the unchanged phase. In itself this inversion provides the confirmatory evidence that the new phase now described has essentially the composition Ca_2SiO_4.

A variety of bredigite exhibiting distinctive features is met with in two or three specimens of the melilite-rocks which have originated by soaking of the chalk by the igneous magma already made alkaline by assimilation (Tilley, 1931). These rocks, as described, carry large plates of honey-coloured melilite, and in the few examples now referred to, the chief additional primary minerals in close association with the bredigite are coarse-grained braided larnite, perovskite, and magnetite. The distinctive feature of the bredigite is its colour and pleochroism. In thicker sections a common pleochroism scheme is as follows: α pale violet, β and γ colourless to palest green. Absorption $\alpha > \gamma > \beta$. The refractive indices measured on a coloured grain gave the values:

$$\alpha\ 1{\cdot}725,\ \beta\ 1{\cdot}728,\ \gamma\ 1{\cdot}740,\ \text{and}\ 2V_\gamma = 33°.$$

Twinning, both multiple and cyclic, on the same law as described is characteristic (pl. XVI, fig. 2). Occasionally twinning on (110) may be associated with the prevalent (130) type. Cleavage is poorly developed, but when present is of the prismatic type (60°). Between crossed nicols

the mineral may show anomalous interference tints, these being particularly evident in sections cut nearly normal to the acute bisectrix. Such sections may exhibit a greenish to purplish tint in place of the normal grey of the first order. Dispersion of the optic axis, $r < v$, is noticeable. The optic axial angle shows considerable variation, values as low as 10° being recorded though these are very exceptional. The mineral behaves like normal bredigite in dissolving readily in weak acid without effervescence and in leaving a silica residue. Besides a microchemical reaction for calcium (very abundant), it yields a strong ferrocyanide test for iron. The distinctive optical properties noted above are doubtless to be ascribed to solid solution, and the unusual paragenesis suggests that, in addition to iron, titanium probably enters in small amount in its composition.

Braided larnite of the melilite-rocks.

The braided larnite of the melilite-rocks differs from normal larnite by its coarse structure—a complex set of lamellae in place of, or in addition to, the very fine parallel system of twin lamellae seen in sections of the latter cut perpendicular to the acute bisectrix (pl. XVI, figs. 1 and 4). The broader lamellae of the former (0·004–0·01 mm. in breadth) are best seen in sections cut normal to the axis β. At least three sets can be distinguished, a double set intersecting at angles close to 60° and a third set bisecting the acute angle between the former. In the cutting position noted the three sets extinguish at very small angles to one another and they stand inclined at high angles to the section; the acute bisectrix (γ) of the group lies in, and almost bisects, the obtuse angle between the double set of lamellae. In ordinary light the lamellae are outlined by thin transparent films and minute opaque granules which define their boundaries and emphasize the structure. Like bredigite the complex may show a pale violet colour and pleochroism, but these features are not constant and both may be confined to particular sets of lamellae within the complex. The structural features noted above present much similarity to those described by Sundius (1933) for one variety of calcium orthosilicate of cement clinker, and they recall the illustrations of clinker orthosilicate quenched from 1450° C. which are provided by Insley (1936, fig. 9, type I Ca_2SiO_4; also 1938, p. 360, fig. 1, type Ia) in his study of the constituent phases of Portland cement.

Sections of braided larnite cut effectively normal to the acute bisectrix show characteristically a low interference tint, and, in accordance with the orientation noted in section normal to β, yield in part a set of sub-

parallel lamellae with positive elongation and the optic axial plane across the length of the lamellae. Individual lamellae may be traced out by rims of opaque granules as seen in the sections normal to β. There are, however, other sections showing a similar low interference tint which exhibit a seemingly confused extinction seen, however, under high power to result from the presence of irregular bands and patches with differing extinction but having in common the γ direction emerging normally from their sections. These show the exceedingly fine twin lamellae (often a double set at right angles) distinctive of larnite. Three group orientations of these units of the aggregate can be distinguished and recognized by the traces of the optic axial planes and the courses of the twin striae. The three groupings make angles of approximately 60° with each other, the relationship being illustrated in text-fig. 2.

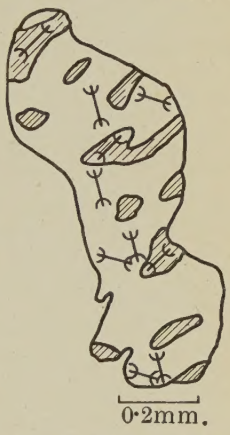

FIG. 2. Inversion intergrowth of braided larnite in a melilite-rock, showing the grouping of the parts into three sets, each with the acute bisectrix normal to the section, but with the mean optic axial plane directions of the sets inclined at 60° to one another. Only one of the triple sets is shown in full development.

The lamellar structure of braided larnite is clearly one of considerable complexity and not yet completely resolved. It has all the characteristics of an inversion product occurring in the form of grains within melilite or intimately associated with bredigite. The two minerals may show in part a common extinction. The braided areas appear in places to eat into the boundaries of the bredigite or the latter may appear like isolated residuals in a base of this structure. Such residuals may be distinguished under high power in sections like text-fig. 2, then appearing as rounded or wedge areas of very low birefringence between the larnite sets noted, and cut normal to the acute bisectrix. On the other hand, though the feature is not common, very thin lamellae of larnite with the characteristic fine twin striae may be seen developing and coursing through grains of twinned bredigite. A striking example is depicted in text-fig. 3, where the orientation of the lamellae and their twin striae (nearly parallel to α) are shown in relation to the twinned parts of a basal section of bredigite. The mutual relations give indeed strong grounds for the interpretation of much at least of this complex as an inversion product of bredigite itself, the films and opaque granules delineating the lamellae of the complex representing material exsolved

on inversion (pl. XVI, figs. 1, 3, 4). Another possibility must be kept in mind. An apparently similar structure is known to result from inversion of an α hexagonal modification of Ca_2SiO_4, as shown in the experiments of Greene (1944) on the inversion of an artificial α-Ca_2SiO_4 solid solution (1944, p. 5, and figs. 4A, 4B) and it remains uncertain whether some of the braided larnite of these rocks has not inverted from an α hexagonal phase now completely transformed.

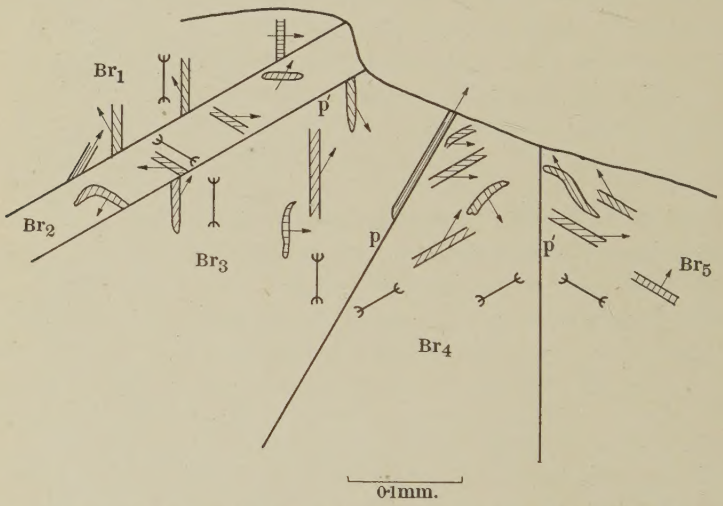

FIG. 3. Inversion lamellae of larnite in a twinned crystal of bredigite. The basal section of bredigite shows repeated and cyclic twinning on p' (130) and is also twinned on p (110) (Br_1–Br_5).

The larnite lamellae likewise have the acute bisectrices perpendicular to the section and are resolved in the bredigite twin into three groups at 60° as indicated by the fine striae and arrow lines—twin edge directions in the several lamellae.

At the right edge of sector Br_5 (but not shown in the sketch) a γ-Ca_2SiO_4 inversion of bredigite is seen superimposed on the larnite type of inversion. The bunched γ-Ca_2SiO_4 fibres stand perpendicular to the section, their orientation relative to bredigite being such that the $\gamma\beta$ plane of γ-Ca_2SiO_4 is very nearly parallel to the optic axial plane of bredigite in this sector, and therefore nearly parallel to a $\beta\gamma$ plane of one of the lamellar sets of larnite.

Bredigite, whether in the normal contact-rock or in the melilite types, gives no indication that it itself has inverted from an α hexagonal phase. The broad and often simple twin structure is that characteristic of a primary orthorhombic form: it does not resemble, for instance, the complex fine twinning seen in β-K_2SO_4 inverted from the α hexagonal K_2SO_4 phase crystallized from the melt.

Braided larnite is not seen in the normal contact-rocks, and there the

only inversion of bredigite recognized is to the γ phase. The origin of the fine multiple twinning of normal larnite is not clearly established. Though suggestive of inversion twinning it should be remarked that this structure can be reproduced in the laboratory with material that has never been subjected to a temperature of 1420° C. The type II Ca_2SiO_4 (of Insley) produced by quenching from 1375° C. appears to correspond to normal larnite (Insley, 1936, fig. 10), and the structure may occur in orthosilicate synthesized at even lower temperatures.

In the original description of larnite it was shown that different specimens of this phase showed great differences in tendency to invert. Some examples were so susceptible to inversion that transformation could be accomplished by the blow of a hammer; others, on the contrary, could be subjected to severe thermal or mechanical treatment without sign of inversion. Laboratory investigations on the capacity of β-Ca_2SiO_4 to invert have shown that the presence of material in solid solution in the phase may have a marked effect on its inversion tendency, some material increasing that tendency, other material stabilizing the phase. It is remarkable that the larnite associated with the bredigite in the normal larnite-rock may show less tendency to inversion than bredigite itself. This is clear from the descriptions already given and from the illustrations of pl. XV. Not infrequently twinned grains of uninverted larnite may be enclosed in the larger grains of the new phase already exhibiting partial inversion to the γ phase.

The γ inversion product of larnite itself may show, as in the case of the bredigite inversion, a regular orientation with the uninverted parent. In such case the fibre direction of the γ phase stands approximately parallel to the acute bisectrix of the larnite.

The orientation relations of the phases produced by inversion in these Scawt Hill rocks may now be summarized:

α'-Ca_2SiO_4 (bredigite)$\rightarrow$$\beta$-$Ca_2SiO_4$ (larnite). $\gamma \parallel \gamma$.

α'-Ca_2SiO_4 (bredigite)$\rightarrow$$\gamma$-$Ca_2SiO_4$. $\gamma \parallel \beta$, $\alpha \parallel \gamma$ nearly.

β-Ca_2SiO_4 (larnite)$\rightarrow$$\gamma$-$Ca_2SiO_4$. $\gamma \parallel \beta$, $\alpha \parallel \alpha$ nearly.

It is hoped that further study of the intimate growth relations of the three phases (α', β, and γ) will, in the light of X-ray data yet to be obtained on single crystals of the bredigite phase, add materially to the evidence now available.

The slag mineral.

The spiegeleisen slags containing the calcium orthosilicate phase came from Middlesbrough and have been for many years in the slag collection

at Cambridge. As a group these slags range from comparatively coarsely crystallized varieties to others largely glassy. The glassy examples are greenish in colour and a greenish hue is imparted even to the crystalline types. This colour is due to the disperse distribution of a calcium sulphide phase coloured green through the presence of manganese.

Apart from glass in variable amount the constituent phases are melilite, the Ca_2SiO_4 phase, a monticellite solid solution, and the ubiquitous calcium sulphide. While melilite is constantly present in bulk, the proportions of the Ca_2SiO_4 phase and monticellite vary greatly. In some, monticellite is almost wholly absent, in others it is the dominant phase, and the Ca_2SiO_4 phase may be present in very subordinate amount.

In those slags rich in the new phase, the mineral appears as elongated hexagonal prismatic crystals, showing prominent development in the interspaces between the melilite tables. It has, however, begun to crystallize early appearing as a fine dendritic growth in the cores of the melilite crystals, or as skeletal crystals in parallel position in the same environment. The periphery of the melilites may be wholly free from inclusions, but idiomorphic prisms of the new phase may occur in this position as well as in the melilite interspaces. When monticellite is present it occupies a similar position as sheaves of crystals, though shreds of it may appear in the core and at the periphery of the Ca_2SiO_4 phase.

The sulphide phase, usually green in colour, forms arborescent growths in the chief phases and as independent grains in the interstitial ground.

A typical spiegeleisen slag, rich in the new orthosilicate phase is figured on pl. XV, fig. 3.

Monticellite has the usual habit of this mineral in slags, elongated parallel to the a-axis and showing edges of the forms k (021) and b (010) in cross-section. It has the high birefringence of a monticellite solid solution containing either iron or manganese or both and the cross-sections show the emergence of γ the obtuse bisectrix.

For the isolation of the new orthosilicate phase a slag containing only traces of monticellite was chosen in order to facilitate a clean separation devoid of another orthosilicate phase. The slag selected was rich in the new phase and showed a sulphide phase, light brown in colour and believed to contain but little manganese. In addition to melilite, the remaining phase was a brown glass present only in small amount. This slag itself was subjected to analysis and the results are set down in table I,

column 1. It shows a comparatively low content of MnO, negligible iron oxide, and a significant content of BaO. The origin of the barium in this slag must be traced to the manganese ore used in smelting, possibly minerals of the psilomelane group in which barium is often an essential constituent.[1] The presence of barium has necessitated consideration of its partition between the sulphide and silicate phases as noted below.

The preponderant mineral of the slag is the orthosilicate phase, melilite being subordinate. The mineral was isolated from melilite by repeated fractionation in the centrifuge, but owing to the fine state of dispersion of the sulphide, this could not be completely eliminated from the final product, which contained in addition a little brown glass. The analysis of the mineral thus far purified is given in table I, column 4.

The final product of separation obtained from centrifuging had a specific gravity of $3{\cdot}40 \pm 0{\cdot}02$. Some of the grains contained minute drops of sulphide and there was in addition a little glass. Microchemical tests showed that the orthosilicate and the small amount of sulphide dissolved in the weakest acids, though the glass remained unattacked in this treatment. The analysis was therefore made of a dilute acetic acid extract representing the orthosilicate and included sulphide. Separate determinations were made of sulphur and the ratio of CaS:BaS in the sulphide enabling the barium content of the orthosilicate to be determined after deducting Ca and Ba in the sulphide of the analysis. A few minutes' extraction in cold 5 % acetic acid followed by treatment with dilute Na_2CO_3 to dissolve the separated silica served to isolate the pure orthosilicate and sulphide from the glass impurity. The last was weighed and represented 4·55 % of the total mineral analysed. In the acetic acid extract all the constituents except water and sulphur were determined.

To derive the figure of barium in the orthosilicate it was necessary to determine its distribution relative to calcium in the sulphide phase. It had been noted early in the centrifuge separation that the sulphide

[1] This analysis is probably exceptional among the group available for study (from the former firm of Messrs. Bolckow and Vaughan, Ltd., Middlesbrough) in its low content of MnO and high figure for BaO. A comparison of available analyses of ferromanganese and spiegeleisen slags shows that they vary considerably in bulk composition. Manganese, however, is consistently higher and BaO much less, though figures of 2 % and over for the latter constituent are on record. The variation in chemical and mineral composition of these types of slags is clearly dependent not only on the character of the primary manganese ore but also on the flux, whether limestone or dolomitic limestone.

TABLE I. Chemical analyses of slag and isolated bredigite.

	1.	2.	3.	4.	5.	6.		
SiO_2 ...	27·04	30·34	32·39	29·96	33·08	5513	1	
Al_2O_3 ...	8·56	9·60	—	nil	nil	—		
TiO_2 ...	0·23	0·26	0·36	0·31	0·34	—		
Fe_2O_3 ...	0·29	0·32	0·44	0·11	0·12	—		
MnO ...	3·02	3·39	4·67	3·06	3·38	476	0·086	2·068
CaO ...	45·71	44·65	46·94	47·53	49·23	8791	1·594	
BaO ...	6·09	5·22	7·19	7·12	6·91	450	0·081	
MgO ...	5·19	5·82	8·01	6·14	6·78	1695	0·307	
Na_2O ...	0·36	0·40	—	—	—			
K_2O ...	nil	—	—	—	—			
H_2O+...	0·70	—	—	0·29	—			
CO_2 ...	0·22	—	—	—	—			
F ...	0·31	—	—	0·14	0·16			
SO_3 ...	0·32	—	—	—	—			
S ...	3·13	—	—	1·86	—			
Insol. ...	nil	—	—	4·55	—			
	101·17	100·00	100·00	101·07	100·00			
Less O = S,F	1·69			0·99				
	99·48			100·08				

1. Spiegeleisen slag, Middlesbrough. P_2O_5 trace, Cr_2O_3 nil.

2. Spiegeleisen slag, recalculated after removal of water, SO_3 and CO_2 as $CaSO_4$ and $CaCO_3$, F as CaF_2, and S allotted to Ca and Ba as CaS 6·37, BaS 1·59.

3. Spiegeleisen slag with gehlenitic fraction of melilite removed as $Ca_2Al_2SiO_7$ and Na in $CaNaAlSi_2O_7$.

4. Bredigite, isolated from slag.

5. Bredigite, recalculated after allotting sulphur to Ca and Ba as CaS 3·78, BaS 0·95, and removal of insoluble.

6. Molecular ratios of bredigite $(Ca_{1·59}, Ba_{0·08}, Mg_{0·31}, Mn_{0·09})$ $[SiO_4]$.

phase had a noticeably greater specific gravity than that recorded for pure CaS (2·6), and it became clear when barium was recorded in the analysis that the higher values obtaining for the specific gravity of the sulphide were to be traced to BaS in solid solution. Microchemical tests established barium in both silicate and sulphide phases. Single grains of the silicate when treated with dilute acetic acid and potassium chromate yielded the characteristic crystals of $BaCrO_4$ which covered the dissolving mineral and became entangled in the silica pseudomorph left by dissolution. Isolated grains of sulphide showed a similar $BaCrO_4$ precipitate but less abundantly. As the use of acids to separate sulphide was excluded, the method adopted was extraction of the sulphide by water in the absence of air and carbon dioxide. Both calcium and barium sulphides react with water to form soluble hydrosulphides, the latter very readily. The finely ground impure orthosilicate was leached

with water over a period of three days, this extraction removing up to 3 % by weight of the material. Microscopic examination of the residue indicated that free sulphide had gone into solution. The virtual absence of silica in the aqueous extract and the character of the silicate grains indicated that no appreciable attack of the silicate phase had taken place under this treatment. From several estimates the average figure of CaS:BaS = 4:1, determined from the content of Ca and Ba in the extract, was obtained. No great accuracy can be claimed for this estimate, but it is to be noted that the correction to any error in the determination, owing to the greater solubility of BaS in water, would result in more Ba being allotted to the silicate phase than has been done using the determined ratios. It is believed, however, that the allocation of BaO to the silicate phase is not in error by more than one-half of one per cent. The molecular ratio $(CaO+BaO):SiO_2$ is of course unaffected by any inaccuracy in the determination of the partition of Ba and Ca between the two phases. With distribution of barium, determined in the sulphide as indicated, the composition of the silicate phase was recalculated to the figures given in column 5 of table I.

It is to be noted that a small content of F (0·14 %) is recorded in the analysis. This small amount of fluorine may of course be replacing oxygen in the mineral, but as its amount is relatively insignificant it has not been considered in the calculation of molecular proportions given in column 6 of table I.

The resultant figures, considering the analytical complexity, reveal reasonably good accord with an orthosilicate ratio. The mineral is thus clearly a calcium orthosilicate with Ca partly replaced by Mg, Mn, and Ba.

The analysis presented in column 5 (table I) may be compared with that of the recalculated slag (column 3). The figures in this column have been derived from the slag analysis by removal of CaS and BaS (in the ratio 4:1) and after removal of all alumina as gehlenite ($Ca_2Al_2SiO_7$) and the hypothetical melilite ($CaNaAlSi_2O_7$)—thus removing also the soda. The close approximation of the two sets of figures (columns 3 and 5) shows that the melilite phase is essentially a gehlenite though probably containing a small percentage of MgO to which also the glass and the rare monticellite would contribute to the total of the slag. Further, that the great bulk of the BaO in the silicate fraction of the slag is contained in the calcium orthosilicate phase. Calculated in terms of phases the slag has approximately 60 % orthosilicate phase, 25 % melilite, 8 % sulphide, and minor glass and monticellite traces.

In text-fig. 4 the composition of the orthosilicate solid solution is plotted in the triangle (Ca,Ba)O–(Mg,Mn)O–SiO_2 to show its position in relation to other phases recognized in slags or dry melts. The extended solid solution it exhibits brings it closest in composition to merwinite, a phase which is not recorded in any of these spiegeleisen slags and which is readily differentiated from the new phase by its distinctive optical properties.

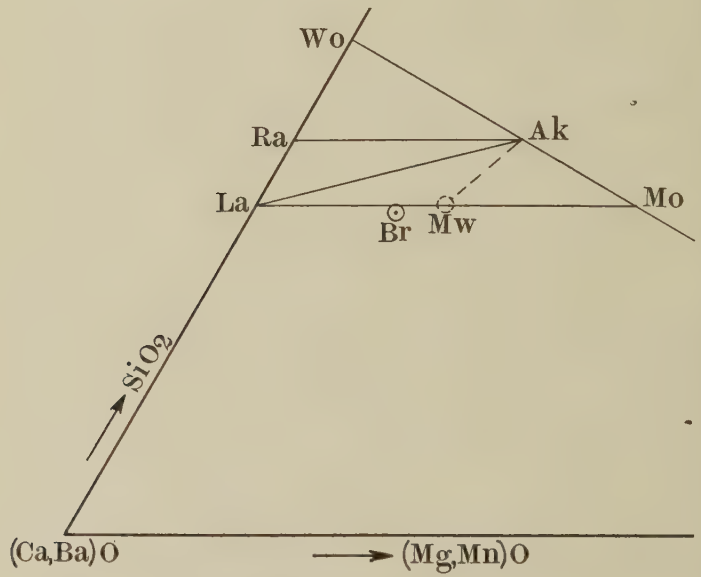

Fig. 4. Composition of the bredigite phase in the slag in relation to the composition of other phases in the system CaO–MgO–SiO_2 (here (Ca,Ba)O–(Mg,Mn)O–SiO_2).

Br bredigite solid solution, La Ca_2SiO_4, Mw merwinite, Ak åkermanite, Ra rankinite, Wo (pseudo)wollastonite.

Properties of bredigite from the slag:

The occurrence of the mineral as elongated hexagonal prisms in the slag has already been described. This characteristic habit is also indicated in pl. XV, fig. 3, where several cross-sections of these prisms, hexagonal in shape, are visible. The habit is thus somewhat contrasted to that of the mineral in the Scawt Hill rocks.

Cleavage is by no means characteristic, but is recorded in one slag. Here the typical 60° prismatic cleavages are met with as in the Scawt Hill mineral.

The basal hexagonal sections show the emergence of the acute bisectrix (γ).

Twinning is very characteristic both of multiple and sector type. An example of repeated twinning seen in a basal section is shown in the accompanying text-fig. 5 and the optical orientation of the twinned parts conforms to the data on the natural mineral.

The refractive indices determined on the material analysed are α 1·713; β 1·717; γ 1·732.

The optic axial angle shows some variation in the sections examined in the various slags. A common value is $2V_\gamma = 30° \pm 2°$, but lower values of 20° are recorded.

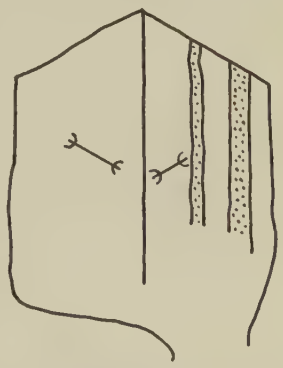

Fig. 5. Basal section of bredigite from the slag showing the repeated twinning and the optical orientation in the twinned parts.

X-ray powder photographs of the slag mineral show a pattern distinctive from those of larnite and merwinite. The photographs are closely similar to those obtained from a synthetic Ca_2SiO_4 prepared by Rait and Goldschmidt (1945) by quenching in water from 1790° C., a specimen of which was kindly presented to us by Mr. H. J. Goldschmidt. Optically the synthetic material resembles the slag phase in being biaxial, optically positive with a similar small optic axial angle, but with slightly lower refractive indices. Further X-ray data will be available when single crystals isolated from one of the spiegeleisen slags have been subject to detailed analysis.

The reluctance of the slag bredigite to invert has already been noted, but there are clear indications in one of the slags that inversion phenomena do occur. These reproduce the features met with in the natural mineral in that fibres of a γ form appear in some of the bredigite grains and yield a characteristic pattern in the basal sections. In general, however, the slag mineral is unaltered and the slags show no macroscopic signs of dusting or falling. It will be clear from a survey of the collective studies made to date on the four modifications of Ca_2SiO_4 (α, α', β, γ) the complications that invest a study of their equilibrium relations. While the capacity they show for solid solution is in great measure responsible for this complexity, there, nevertheless, remain for pure Ca_2SiO_4 problems of phase relationship, particularly of higher forms, which only further experimental work can hope to solve.

References.

Bredig (M. A.), Journ. Amer. Chem. Soc., 1941, vol. 63, p. 2533.
—— Journ. Phys. Chem., 1942, vol. 46, p. 747.
—— Amer. Min., 1943, vol. 28, p. 594. [M.A. **9**–92.]
Day (A. L.) and Shepherd (E. S.), Journ. Amer. Chem. Soc., 1906, vol. 28, p. 1104.
Greene (K. T.), Journ. Research Nat. Bur. Standards U.S.A., 1944, vol. 32, p. 1.
Hansen (W. C.), Journ. Amer. Ceram. Soc., 1928, vol. 11, p. 68.
Insley (H.), Journ. Research Nat. Bur. Standards U.S.A., 1936, vol. 17, p. 357.
—— *et alii*, ibid., 1938, vol. 21, p. 355.
Rait (J. R.) and Goldschmidt (H. J.), Journ. Iron and Steel Inst., 1945, vol. 151 (no. 1 for 1945), p. 429.
Rankin (G. A.), and Wright (F. E.), Amer. Journ. Sci., 1915, ser. 4, vol. 39, p. 7. [M.A. **1**–320.]
Schleede (A.), Angewandte Chem., 1940, vol. 53, p. 65.
Sundius (N.), Zeits. anorg. Chem., 1933, vol. 213, p. 343.
Taylor (W. C.), Journ. Research Nat. Bur. Standards U.S.A., 1941, vol. 27, p. 311.
Tilley (C. E.), Min. Mag., 1931, vol. 22, p. 457.
Trömel (G.), Stahl und Eisen, 1943, vol. 63, p. 21.
Van Valkenburg (A., *Jr.*) and McMurdie (H. F.), Journ. Research Nat. Bur. Standards U.S.A., 1947, vol. 38, p. 415.

Explanation of Plates XV and XVI.

Plate XV.

Fig. 1. Spurrite-rock, Scawt Hill, Co. Antrim. ×15 diameters.

Showing a large plate of spurrite enclosing turbid boat-shaped grains of bredigite, some partially inverted (dark areas within the grains represent the fibrous development of γ-Ca_2SiO_4). Little cubes of magnetite and minute drops of larnite are present as inclusions in the spurrite.

Figs. 2 and 4. Spurrite-larnite-rock, Scawt Hill. ×22 diameters. Fig. 2 in ordinary light, fig. 4 crossed nicols.

In fig. 2: below, granular larnite with some bredigite; above, clear spurrite. The central crystal is a hexagonal twinned cross-section of bredigite. In the spurrite are other grains of bredigite and numerous drop-like grains of larnite.

Fig. 4 shows the twinning of the central grain of bredigite with a drop-like grain of twinned larnite showing at the centre (white).

Fig. 3. Spiegeleisen slag, Middlesbrough. ×15 diameters.

Melilite tables with turbid cores and clear peripheries. The cores of the melilites are filled with elongated drop-like grains of bredigite. Between the melilite crystals well-shaped pseudo-hexagonal prisms of bredigite. A cross-section is seen immediately to the left of the central vug and a prismatic section on the SE. edge of the vug. Numerous other prisms of bredigite are visible. Green calcium sulphide (dark) as arborescent growths and some associated bredigite.

Plate XVI. Melilite-bredigite-larnite assemblages of Scawt Hill, Co. Antrim. ×15 diameters.

Fig. 1. The central crystal with straight edges is bredigite showing on its ragged SW. edge the development of braided larnite (as an inversion structure).

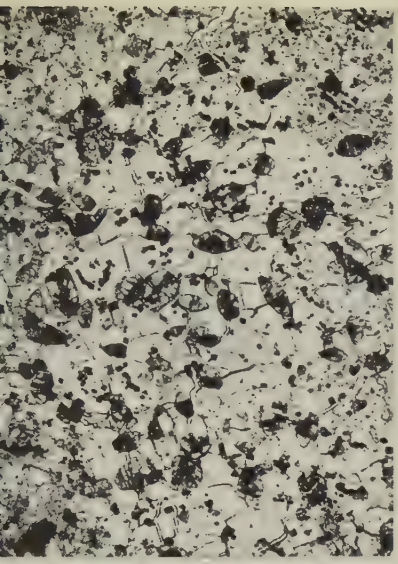

1

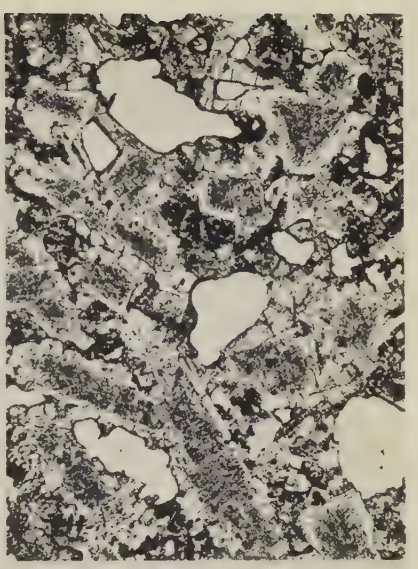

3

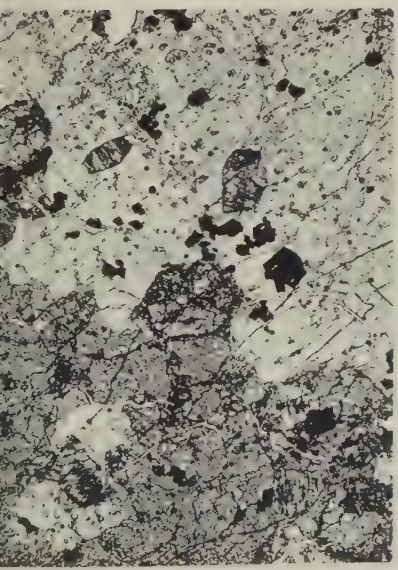

2

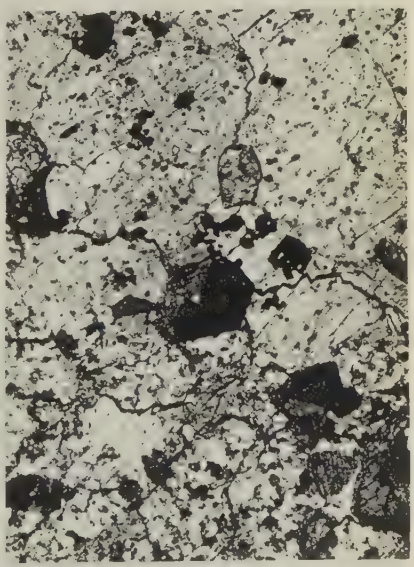

4

C. E. Tilley & H. C. G. Vincent: Bredigite.

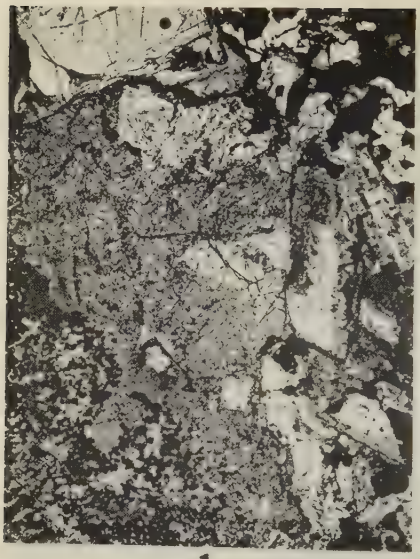

1

3

2

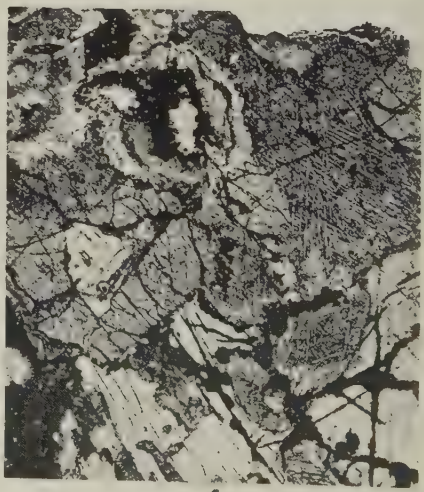

4

C. E. Tilley & H. C. G. Vincent: Bredigite.

More braided larnite is seen above and to the left. Clear areas are mostly melilite. In the SW. corner a zone of normal larnite rock with magnetite and some spurrite. A hexagonal cross-section of bredigite is seen NNE. of the central bredigite crystal.

Fig. 2. Centre, a sector twin of bredigite cut nearly $\perp$ to Bx_a; cross-sections of melilite (laths); below, bredigite (white) partly enwrapping a lath section of melilite at extinction. Crossed nicols.

Fig. 3. Lower centre, a subidioblastic crystal of bredigite with prismatic cleavage (vertical section), enveloped by melilite; left above, an inverted grain (braided larnite); melilite (lath sections), dark areas include perovskite. Below, rounded grains in melilite now inverted to braided larnite.

Fig. 4. Above right, a large area of braided larnite showing the typical lamellae (3 sets visible). The remainder of the photograph shows chiefly bredigite and melilite with some perovskite.

Earlier stages in the metamorphism of siliceous dolomites.

(With Plates XVII and XVIII.)

By C. E. Tilley, F.R.S.

Department of Mineralogy and Petrology, University of Cambridge.

[Read November 6, 1947.]

In the progressive thermal metamorphism of siliceous dolomites, tremolite and calcite are usually considered the earliest of the new mineral phases formed by reaction of the primary materials, dolomite and quartz. An early formation of forsterite has also been recorded, as, for example, in the dolomitic zones of the Durness limestone surrounding the Tertiary Beinn an Dubhaich granite of Skye. In this aureole, however, the relation of forsterite to tremolite has hitherto not been closely investigated. As Bowen[1] has pointed out in his systematic study of the progressive metamorphism of siliceous limestones and dolomites, a first formation of forsterite from dolomite and quartz could not rank as an equilibrium reaction since forsterite and quartz can have no stable coexistence. Tremolite has accordingly been regarded as the first metamorphic product in an equilibrium series of reactions of increasing decarbonation affecting siliceous dolomites in an advancing higher temperature environment at any given pressure. In the Broadford–Kilchrist area of Skye, the Cambrian dolomites belong particularly to horizons known locally as the Beinn an Dubhaich and Strath Suardal zones. Those in the inner aureole of the granite provide spectacular examples of high-grade metamorphism which has been detailed by Harker[2] in the Skye memoir. Outcrops of dolomite in the outer aureole of this intrusion providing data on earlier stages of alteration occur in the area east of Ben Suardal where bands of the Strath Suardal zone are brought up by folding and thrusting and are enveloped by the Ben Suardal limestone zone (a^{VI}) of the Durness group. This zone of dolomite forms a band running NNE. from $\frac{1}{2}$ mile NE. of the summit of Ben Suardal to a point nearly $\frac{1}{2}$ mile south of the same position. At the north end of the outcrop the dolomite is approximately one mile from

[1] N. L. Bowen, Journ. Geol. Chicago, 1940, vol. 48, pp. 225–274. [M.A. 8–243.]

[2] A. Harker, The Tertiary igneous rocks of Skye. Mem. Geol. Surv. Scotland, 1904, pp. 144–151.

the nearest exposed granite and the south end approaches to a distance less than $\frac{3}{4}$ mile from the granite.

The Strath Suardal zone is characterized by chert nodules and lumps an inch or two across which resemble sponge forms but show no clear organic structure, and it is at the contact of the dolomite with these chert nodules that the first signs of metamorphism involving the production of new minerals are found. Examination of numerous specimens from this band of the Strath Suardal dolomite makes clear that *talc* is the first new-formed phase to be recognized and its formation is therefore to be ascribed to reaction between dolomite and quartz.[1] The chert forms become invested with a thin dense white unctuous skin which microscopic examination reveals as talc (pl. XVII, figs. 1 and 2).

At the north end of the outcrop a few examples were studied in which there were no signs of reaction between the carbonate and chert, but the great majority show the production of one or more new mineral phases.

In the earliest stage talc then appears immediately adjacent to chert as fine flakes together with calcite forming the skin referred to above. In a more advanced stage of talc development the talc zone can be divided into two or more sub-zones: (1) an inner zone against the chert built up of relatively coarse-grained talc, quartz, and calcite, the grain size of the quartz being often notably coarser than that in the interior of the nodule; (2) a fine-grained zone, rich in talc but associated with fine granular calcite which gives turbidity to this zone; (3) an outer coarse zone with subordinate talc associated with calcite and dolomite. In the dolomite ground which invests these zones sparse flakes of talc can be recognized adjacent to the contact. Their presence is readily made out if a thin section of the rock is treated with acid to remove the dominant carbonate. Talc also occurs in the body of the chert either in irregular areas or forming with calcite pseudomorphs after former idioblastic rhombohedra of dolomite.

The distribution of the three zones just described is depicted in pl. XVIII, figs. 1 and 2.

In still more advanced stages tremolite appears as a new phase. Its incoming is associated with the inner zone where quartz, calcite, and talc are intimately associated. The tremolite appears as diversely arranged prisms—sometimes more regularly set at right angles to the surface of the chert form, and they spring into the fine turbid zone of

[1] The associated Ben Suardal limestone containing black cherts (quartz-calcite association), unless partially dolomitized, shows no new mineral phase development at the stages here considered.

talc (zone 2) which follows. The distribution is seen in the photomicrograph 3 of pl. XVIII. Numerous examples of chert surrounded by a tremolite zone fringed towards the dolomite groundmass by a talc zone in which incipient tremolite spears are developing are to be found in these dolomite outcrops. Ultimately the talc zone itself disappears and is replaced by a tremolite zone. In the inner zones of the aureole talc is found only as a retrograde mineral and is then readily recognized in the form of pseudomorphs after tremolite and also olivine. Retrograde talc is also found though sparingly in the tremolite-bearing zones of the outer aureole.

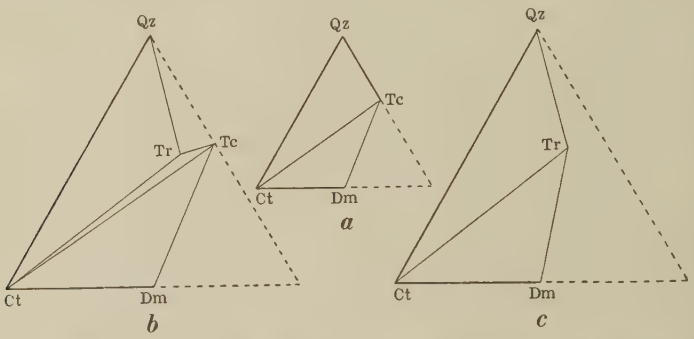

Fig. 1. Projection of the CaO–MgO–SiO_2–CO_2 tetrahedron to show earlier stages of metamorphism.

Ct calcite, Dm dolomite, Qz quartz, Tc talc, Tr tremolite.

In the outer band of dolomite now described, talc and tremolite are the dominant new mineral phases, and their mutual relations make clear that talc is the initial product in the metamorphism.

Of about 50 specimens showing chert nodules collected from this band of the outer aureole only two were found to contain no new mineral phase at the contact of dolomite and chert. Talc is a constituent of the great majority, about 50 % showing talc alone. Of the rest the major number show both talc and tremolite. Only two specimens showed the presence of diopside (associated with tremolite) and one of these exhibited sparse forsterite with tremolite in the dolomite groundmass.

Forsterite and diopside are to be recognized as products of higher grades, but the onset of reactions producing them here is doubtless to be ascribed to conditions permitting reduction in the pressure of CO_2, perhaps through circulating solutions. The rare development of these two phases shows that this condition was only locally reached. The production of talc and tremolite, the predominant new mineral phases

of the outer aureole, can be ascribed to a series of reactions of increasing decarbonation. They are as follows:

(*a*) 3 Dolomite + 4 Quartz + H_2O ⇌ 1 Talc + 3 Calcite + $3CO_2$. Many of the rocks belong to this stage of metamorphism (assemblages talc-calcite-quartz, talc-calcite-dolomite).

This reaction involving water, one of five components, has the attributes of a univariant equilibrium, as Bowen has shown in his discussion of a *first* formation of tremolite, if a liquid solution is postulated as present (6 phases). The simplified treatment using the 'dry' formula for talc (and diagrammatically portrayed) implies the absence of a participating liquid phase, and the condition of univariancy may be considered unchanged.

(*b*) 5 Talc + 6 Calcite + 4 Quartz ⇌ 3 Tremolite + $6CO_2$ + $2H_2O$, leading to the initial formation of tremolite with associations tremolite-talc-calcite; tremolite-calcite-quartz of the inner zone depicted in pl. XVIII, fig. 3.

(*c*) 2 Talc + 3 Calcite ⇌ 1 Tremolite + 1 Dolomite + CO_2 + H_2O.

These three stages are graphically depicted in text-fig. 1 (*a*, *b*, *c*) which presents a projection of the quaternary system CaO–MgO–SiO_2–CO_2, with the phases talc and tremolite represented by their anhydrous formulae ($3MgO.4SiO_2$ and $2CaO.5MgO.8SiO_2$ respectively). The successive assemblages formed in the three stages correspond to the succession of overlapping planes in the tetrahedral figure met by lines proceeding from the CO_2 apex. It is of interest to note that the production of tremolite in reaction (*c*) leads to the reformation of dolomite.

Neither enstatite nor anthophyllite appear to be formed during the metamorphism of siliceous dolomite though they are possible members of assemblages in a successive decarbonation series. Unlike talc, however, they appear to be unstable in the presence of calcite. Both these phases might be expected to develop from carbonate assemblages of more highly magnesian character than quartz-dolomite associations, e.g. those bearing magnesite.

Explanation of Plates XVII and XVIII.

Plate XVII. Talc surrounding chert in dolomite from Skye.

Fig. 1. Talc envelopes to chert nodules on weathered surface of dolomite: centres of nodules contain calcite and quartz, ½ mile NE. of summit of Ben Suardal. Natural size.

Fig. 2. Talc envelopes to chert nodules in dolomite. A polished slab of the dolomite has been etched and stained (ferrous ferricyanide). Cores of chert (clear) with zone of talc and calcite (stained), fine talc zone (clear),

calcite-talc-dolomite zone at edge (calcite stained). The exposed centres of some nodules are filled with calcite (stained). The mottled dolomite of the groundmass is unstained, $\frac{1}{2}$ mile NE. of summit of Ben Suardal. $\frac{3}{4}$ natural size.

PLATE XVIII. Photomicrographs of talc and tremolite zones around chert in dolomite from Skye.

Fig. 1. Zones around chert nodules in dolomite, nearly $\frac{1}{2}$ mile SE. of summit of Ben Suardal. $\times 25$ diameters.

(1) Chert below,
(2) zone of clear coarse-grained talc with some calcite,
(3) turbid zone of fine talc with some granular calcite passing into coarser zone rich in calcite, dolomite, and subordinate talc,
(4) above, normal dolomite.

Fig. 2. Dolomite with talc zones, $\frac{1}{2}$ mile NE. of summit of Ben Suardal. $\times 20$ diameters.

(1) Below, zone of chert with some talc and calcite replacing it,
(2) narrow fine clear talc zone,
(3) turbid talc zone, fine with some granular calcite,
(4) coarser zone rich in carbonate (calcite and dolomite) with subordinate talc,
(5) normal dolomite.

In the chert zone, original dolomite rhombohedra are seen replaced by talc.

Fig. 3. Dolomite with talc and tremolite zones, $\frac{1}{3}$ mile E. of summit of Ben Suardal. $\times 25$ diameters.

(1) Below, chert, some calcite,
(2) tremolite zone with calcite, some talc or quartz,
(3) above, talc zone with spears of tremolite springing into it from tremolite zone. The talc zone is followed by
(4) normal dolomite not shown in the photomicrograph.

The geochemistry of radiogenic strontium.

By L. H. Ahrens, D.Sc., F.R.I.C.

Research Fellow of the South African Council for Scientific and Industrial Research.

Dept. of Geology, University of the Witwatersrand, Johannesburg, Union of South Africa.

[Communicated by Dr. S. R. Nockolds; read June 26, 1947.]

Introduction.

THE important influence that the radioactive decay of the radio-elements uranium and thorium has had on the geochemical distribution of lead is now well appreciated, but little is known about the possible geochemical implications of the radioactivity of rubidium.

Like its alkali metal homologue potassium, rubidium is β radioactive and slowly disintegrates into a stable isotope of strontium: small quantities of strontium have therefore been accumulating in various minerals since the earth's crust first consolidated. This paper will describe firstly, the abundance of radiogenic strontium in the earth's crust as a whole, and secondly, the distribution of radiogenic strontium in various minerals and rocks, in particular those which are of igneous origin.

Calculation of the amount of radiogenic strontium generated by rubidium.

The disintegration equation for any radioactive element may be written as follows:

$$N = N_o e^{-\lambda t}, \qquad (1)$$

where N_o is the number of atoms originally present and N the number left after a time t has elapsed; λ is the disintegration constant for the particular radioactive element in question. According to Hahn and Walling (1) and Hemmendinger and Smythe (2), in rubidium only the isotope Rb^{87} is radioactive and by losing an electron (β particle) a strontium isotope of equivalent mass number, Sr^{87}, is obtained: in the above equation N_o and N refer therefore to atoms of Rb^{87} and λ to the disintegration constant for Rb^{87}.

The radioactive decay of Rb^{87} is extremely slow and during earth periods only a very small proportion of the total rubidium will have decayed, and for calculations on the radiogenesis of strontium one may regard the quantity of rubidium in any mineral or rock as having remained constant throughout its lifetime. Equation (1) can then be simplified and written as follows:

$$N = N_o - \lambda t N \text{ or } N_o - N = \lambda t N. \quad (2)$$

But $N_o - N$ is the number of atoms of Rb^{87} that have decayed and this number is equal to the number of Sr^{87} atoms generated. Furthermore, Rb^{87} and Sr^{87} have the same mass and equation (2) can be expressed as,

$$\% \text{ radiogenic Sr} = \% \text{ Rb}^{87} \times t \times \lambda. \quad (3)$$

If λ, t, and $\%$ Rb^{87} are known, it is then possible to calculate the quantity of radiogenic strontium present in any material.

The value of λ.—Hahn (3) gives $1{\cdot}1 \times 10^{-11}$ $year^{-1}$ as the value for λ. This value is probably more accurate than previous direct measurements of λ and is based on Pb/U age determinations of certain ancient uranium minerals which were believed to be of the same age as a rubidium-rich mica which was found to contain only radiogenic strontium. A quantitative analysis was made of the rubidium and also of the strontium in the mica, and because the age of the mineral was known, the period of half-life and the disintegration constant for Rb^{87} could be determined.

The value of t.—The absolute geologic ages of some of the specimens described in this paper are believed to be relatively accurate, since the ages of the formations in which the specimens occur have been determined. The ages of other specimens can only be regarded as approximate and have been obtained by interpolating or extrapolating whatever age data are available. However, for this discussion on the radiogenesis of strontium in minerals very accurate age data are not necessary.

Percentage of Rb^{87}.—Rubidium consists of two isotopes only, Rb^{85} and Rb^{87}, the relative abundance of the latter isotope being 27 %. Total rubidium is estimated spectrochemically (ordinary chemical methods are sometimes used) and 27 % of this quantity = $\%$ Rb^{87}.

The abundance of radiogenic strontium in the earth's crust.

To calculate the amount of radiogenic strontium in the earth's crust, t will be equivalent to the time that has elapsed since the formation of the earth. Unfortunately there still is a considerable degree of uncertainty as to the exact age of the earth, although there appears to be

little doubt about the order of magnitude: a value of $t = 3{\cdot}0 \times 10^9$ years will be used here.

Much research is still required before it will be possible to estimate accurately the abundance of rubidium in the earth's crust. Goldschmidt (4) places the concentration at about 0·03 % Rb, whereas I. and W. Noddack (5) give a much lower value. With an increased amount of data at one's disposal, it would seem that the former value is more nearly correct and will be used for calculating the amount of radiogenic strontium in the earth's crust. The approximate abundance of Rb^{87} is thus about 0·0075 %, whence by substituting for t, % Rb^{87}, and λ in equation (3) the abundance of radiogenic strontium in the earth's crust is calculated as 0·00025 %.

The proportion of radiogenic strontium in the total strontium in the earth's crust.

According to Goldschmidt (4) the concentration of strontium in the earth's crust is about 0·04 %, whereas I. and W. Noddack give about one-half of this value. In general there seems to be considerable disagreement on the amounts of strontium found in different rock types, and in this paper the mean of the above two values (0·03 %) will be used. The proportion of radiogenic strontium in the total strontium in the earth's crust is thus approximately $0{\cdot}00025/0{\cdot}03 \times 100 = 0{\cdot}8$ %.

Although the proportion of radiogenic strontium in the total strontium is thus not very considerable, it cannot be regarded as negligible and it will be shown later that in several minerals, particularly in those which have formed from residual pegmatitic emanations, the radioactive decay of rubidium is the chief source of strontium: this follows from the rather different ways in which strontium and rubidium behave during the selective crystallization of magmatic melts and their emanations.

The abundance of radiogenic strontium in minerals of igneous origin.

From equation (3) it is readily seen that most radiogenic strontium will be found in ancient minerals relatively rich in rubidium. Rubidium does not form minerals of its own, but is always present in potassium-rich minerals and also the caesium mineral pollucite (Ahrens, 6); in these minerals Rb^+ (radius 1·49 Å.) is able to replace K^+ (radius 1·33 Å.) and Cs^+ (radius 1·65 Å.) within the lattice.

In potassium minerals the rubidium content varies very considerably and the ratio K/Rb is by no means even nearly constant. Since

potassium and rubidium are almost identical chemically, the inconstancy of the K/Rb ratio is undoubtedly due to the difference in the radii of their respective ions. Goldschmidt (7) has pointed out that because the radius of Rb^+ is appreciably greater than that of K^+, its electrostatic field of attraction is weaker than that of K^+, and hence rubidium tends to be concentrated relative to potassium in the residual crystals of potassium minerals, for example, in those of late formation in pegmatite. Furthermore, the lattices of certain potassium minerals appear to act as more suitable hosts for accommodating the large rubidium ion; available evidence seems to indicate, for example, that Rb^+ can enter the mica lattice with greater facility than it can the felspar lattice.

The ages of several minerals that have been analysed for rubidium are known and the abundance of radiogenic strontium may be calculated: as mentioned before, the ages of some of the specimens can only be regarded as approximate. Calculations on all known analysed (for rubidium) specimens, the ages of which are known, have not been made; and in the following discussion on the abundance of radiogenic strontium in different minerals of known age, in nearly all cases only specimens that have been analysed for total strontium as well as rubidium are described. Without a knowledge of the total strontium content it is not possible to estimate the proportion of radiogenic strontium unless isotope analyses have been made. (See discussion on the proportion of radiogenic strontium in different minerals.)

Lepidolite.—Lepidolite is the mineral richest in rubidium (and hence in radiogenic strontium) and contains on an average 1·5 % Rb, the latitude of variation being about 0·5–3·0 % Rb. Some analyses and calculations on lepidolites of various ages are given in table 1.

Table 1. Amounts of rubidium and radiogenic strontium in lepidolite.

No.	Locality.	Approx. age* (years).	% Rb.	% Rb^{87}.	Calc. % radiogenic Sr.
1.	Pala, California	120×10^6	2·0	0·54	0·0007
2.	„ „	170×10^6	2·0	0·54	0·001
3.	Newry, Maine, U.S.A. ...	300×10^6	1·0	0·27	0·001
4.	Norway, „ „ ...	300×10^6	1·5	0·40	0·0015
5.	Karibib, South-West Africa	800×10^6	1·8	0·49	0·004
6.	„ „ „ „	900×10^6	0·9	0·24	0·0024
7.	Omaruru, „ „ „	1250×10^6	2·4	0·65	0·009
8.	Warmbad, „ „	1050×10^6	1·6	0·43	0·005
9.	Black Hills, South Dakota	1000×10^6	1·3	0·35	0·0037
10.	Kubuta, Swaziland ...	2000×10^6	2·5	0·68	0·015
11.	Manitoba	1900×10^6	2·5	0·68	0·015

* According to Sr/Rb age measurements, with the exception of no. 11.

With the exception of no. 11, all above analyses for rubidium are from Ahrens (8); no. 11 is from Strassmann and Walling (9).

Only in the most ancient of the specimens of lepidolite (nos. 10 and 11) does the concentration of radiogenic strontium exceed 0·01 %; these ancient lepidolites contain about the maximum quantity of radiogenic strontium likely to be found in any mineral.[1]

Amazonite (green microcline).—Amazonites appear to be characteristically richer in rubidium than most other potash-felspars and usually contain 0·1–1·5 % Rb: an average concentration for rubidium in amazonite is about 0·5 %. The calculated concentrations of radiogenic strontium in some analysed specimens of known age are given in table 2.

TABLE 2. Amounts of rubidium and radiogenic strontium in amazonite.

No.	Locality.	Approx. age (years).	% Rb.	% Rb^{87}.	Calc. % radiogenic Sr.
1.	Ilmen Mts., Russia ...	200×10^6	1·3	0·35	0·0008
2.	„ „	200×10^6	2·0	0·54	0·0012
3.	Madagascar	$1000? \times 10^6$	1·3	0·35	0·0038
4.	Pike's Peak, Colorado ...	1050×10^6	1·3	0·35	0·0038

Rubidium analyses nos. 1 and 2 are from Tolmachev and Filippov (10) and nos. 3 and 4 are from Ahrens (11).

Pollucite.—The mean rubidium content of pollucite appears to be about the same as is commonly found in amazonite (Ahrens, 6). Calculated concentrations of radiogenic strontium in some analysed specimens of pollucite of known age are given below (table 3).

TABLE 3. Amounts of rubidium and radiogenic strontium in pollucite.

No.	Locality.	Approx. age (years).	% Rb.	% Rb^{87}.	Calc. % radiogenic Sr.
1.	Norway, Maine, U.S.A. ...	300×10^6	0·23	0·062	0·0002
2.	Greenwood, „ „ ...	300×10^6	0·68	0·18	0·0006
3.	Varuträsk, Sweden ...	$650? \times 10^6$	0·37	0·10	0·0007
4.	Karibib, South-West Africa	1000×10^6	0·54	0·15	0·0017
5.	Black Hills, South Dakota	1350×10^6	0·25	0·067	0·001

The rubidium contents of the above analyses are from Ahrens (6).

In general, the three mineral types discussed above (lepidolite,

[1] The four lepidolite specimens from South-West Africa and the one from Swaziland are from pegmatites associated with the 'Old Granite' of Southern Africa. Little is known about the ages of this 'Old Granite' from different areas, but the available data indicate that 1000×10^6 years may be regarded as an approximate mean age of the 'Old Granite', although it is possible that the Swaziland specimen (No. 10) may be very much older ($\times 2$) than the other 'Old Granite' specimens.

amazonite, pollucite) and probably also hydrothermal microcline other than amazonite, contain higher concentrations of radiogenic strontium than any other mineral.

Muscovite and biotite.—The rubidium content of muscovite and biotite varies very considerably and is in general usually higher than is commonly found in potash-felspar. Pegmatitic muscovites enriched in lithia appear to be enriched in rubidium. For minerals of equivalent age, muscovite and biotite appear to contain as an approximate average 1/5–1/10 of the amount of radiogenic strontium usually found in lepidolite. (See tables 5 and 6.)

Potash-felspar (microcline, orthoclase, and perthite).—Most specimens of potash-felspar appear to contain 0·01–0·3 % Rb, although from some areas felspar may be unusually poor in rubidia (for example, specimens of pegmatitic felspar from the 'Old Granite' near Mid-Illovo, Natal, South Africa, were found to contain usually less than 0·01% Rb), or unusually high (for example, the Varuträsk area in Sweden contains microcline which frequently contains 0·5–2·0 % Rb (12)): in general pegmatitic felspar appears to be richer in rubidium than parent-rock felspar.

Perhaps it is not justified to make a comparison of 'rubidium-rich' and 'rubidium-poor' areas as indicated above, until more data are available, because one important factor, that of phase of mineralization, has to be taken into account. Thus, for example, most microcline found in pegmatite has apparently been formed during the primary consolidation of the pegmatitic base material; sometimes, however, microcline has formed during a later hydrothermal phase, which may be associated with lithianization in the pegmatite, as, for example, at Varuträsk; and from general geochemical principles one would expect a considerable enrichment of rubidium in late hydrothermal microcline of this type. This factor may be an important reason for the relative richness of rubidium in microcline from the Varuträsk pegmatite.

In most cases the amount of radiogenic strontium will be small, and if we assume an average felspar to contain about 0·05 % Rb, then for a relatively young specimen (100×10^6 years) 0·000015 % Sr will be generated; in a medium-aged specimen (500×10^6 years) about 0·00006 % Sr will be generated; whereas about 0·00020 % Sr would be generated in an ancient specimen (1500×10^6 years). These amounts serve to indicate what quantities of radiogenic strontium are likely to be found in potash-felspars of different ages. Reference to the discussion on the proportion of radiogenic strontium in felspar on page 287 will show

quantities of radiogenic strontium found in some specimens of felspar discussed in this paper.

The proportion of radiogenic strontium in the total strontium in different minerals and rocks.

Methods for determining the relative abundance of Sr isotopes.—Of more interest than the absolute abundance of radiogenic strontium is its proportion of the total strontium in different minerals and rocks. Common strontium consists of a mixture of isotopes Sr^{84} (0·6 %), Sr^{86} (9·9 %), Sr^{87} (7·0 %), and Sr^{88} (82·6 %), whereas radiogenic strontium consists only of Sr^{87}. In minerals and rocks the proportion of radiogenic strontium may be determined either indirectly or directly.

In the indirect method the abundance of radiogenic strontium is calculated as before and if the total strontium has been estimated experimentally, the proportion of radiogenic strontium can be calculated. This indirect method can only be regarded as rather approximate because the accuracy with which all factors (λ, t, % Rb^{87}, and % total Sr) are known in any instance is not very great. Nearly all the proportions of radiogenic strontium discussed in the next few pages are based on these indirect determinations.

The usual direct method for determining the isotopic composition of an element, and which may be used for strontium, is analysis by means of the mass spectrograph. Two other methods which warrant investigation in this respect will be mentioned. One method is based on relative intensity measurements on the hyperfine components of suitable strontium lines in line emission spectra of strontium: Heyden and Kopfermann (13) have been able to demonstrate clearly that for the lines they examined, the hyperfine structure patterns for ordinary strontium were quite different from those emitted by pure Sr^{87}, and it follows that in a mixture of ordinary strontium and radiogenic strontium, relative intensity measurements on the hyperfine components of a suitable line should indicate isotopic composition. A third possible method depends on frequency shifts in certain SrF band spectra shown by $Sr^{88}F$, $Sr^{87}F$, and $Sr^{86}F$. Although it may be possible to make isotope analyses of strontium by means of relative intensity measurements on certain SrF band spectra, the procedure will quite likely be excessively tedious.

The above methods for estimating the relative abundance of strontium isotopes depend in each case on slight variations in nuclear mass.

Recently Professor Robley D. Evans of the Massachusetts Institute of Technology suggested (private communication) another possible method for determining Sr^{87} which is based on nuclear configuration and not mass variations. His suggestion will not be discussed here in detail, but briefly it is as follows: Sr^{87} may be excited by non-capture collision to a metastable state of 2·7 hour half-period, whereas other strontium isotopes are not affected; it may therefore be possible to estimate Sr^{87} by making relative intensity measurements of the radiations emitted after bombardment with suitable missiles, for example, with the aid of a cyclotron or a van der Graaff generator.

Relative proportion of radiogenic strontium in lepidolite.[1]—According to Hahn and Walling (1), a mass spectrographic examination of strontium in an ancient lepidolite from Canada showed the strontium to be 99·7 % radiogenic. Further direct corroborative evidence that strontium in lepidolite is essentially radiogenic has been furnished by Brewer (14) who examined strontium in five different specimens and found no evidence of the presence of non-radiogenic strontium.

Data based on indirect evidence indicate that in the specimens of lepidolite referred to in table 1 the proportion of radiogenic strontium is probably between 80–100 %, with the probable exception of the specimen from Swaziland which may contain about 50 %. These results together with the mass spectrographic data show conclusively that in lepidolite radiogenic strontium is invariably predominant, and only minute traces, if any at all, of magmatic strontium are likely to be present.

Relative proportion of radiogenic strontium in amazonite.—No direct isotope analyses have been made on the strontium that is always found in amazonite. Total strontium has been determined on a few specimens of amazonite of known age, and data on the proportions of radiogenic strontium in four specimens of amazonite are given in table 4. The specimen numbers correspond to the specimen numbers in table 2.

In all these specimens the proportion of radiogenic strontium is high and sometimes predominates. An approximate analysis by Oftedal (15) of some pre-Cambrian amazonite from Telemark, Norway, substantiates these findings: about 0·5 % Rb and about 0·01 % Sr were found in the

[1] Since submitting this paper, new information has been published on the proportion of radiogenic strontium in certain minerals. Using the mass spectrograph, J. Mattauch (Angew. Chem., 1947, A, no. 2, p. 37) finds 97·4–>99·7 % radiogenic Sr in lepidolite (four specimens) and 46·3–84·3 % in microcline (four specimens). Although not stated so by the author, it is very probable that all the specimens of microcline he analysed, one of which was the amazonite variety, are *hydrothermal*.

specimen of amazonite, and because it is ancient, a relatively large proportion of the strontium must be radiogenic.

TABLE 4. Relative proportion of radiogenic strontium in amazonite.

No.	% radiogenic Sr.	% total Sr.	Approx. prop. radiogenic Sr.
1. Ilmen Mts., Russia ...	0·0008	0·0015	50 %
2. „ „ ...	0·0012	0·0020	60
3. Madagascar	0·0038	0·01	40
4. Pike's Peak, Colorado ...	0·0038	0·0046	80

Total strontium in nos. 1, 2, and 3 is from Tolmachev and Filippov (10), and in no. 4 from Ahrens (8).

Pollucite.—According to Hahn (3), a mass spectrographic examination of strontium in pollucite from Varuträsk, Sweden, showed it to be largely radiogenic. Indirect evidence on other specimens of pollucite referred to in table 3 indicate strongly that the bulk of the strontium in each of these minerals that has been examined is radiogenic. (See Ahrens, 6.)

Muscovite and biotite.—Recently Nockolds and Mitchell (16) published results of the analyses of several separated micas (all biotites with one exception, no. 12 in table 5) from Caledonian igneous rocks from Scotland. Rubidium and strontium are included in their analytical data, and assuming an age of about 350×10^6 years for these rocks, the approximate proportion of radiogenic strontium in each analysed mineral has been calculated (table 5).

TABLE 5. Amounts of Rb and Sr in Scottish micas.

No.	% Rb.	% Rb^{87}.	% total Sr.	% radiogenic Sr.	Approx. prop. radiogenic Sr.
1.	0·10	0·027	0·01	0·0001	1·0 %
2.	0·15	0·041	0·01	0·00016	1·6
3.	0·15	0·041	0·008	0·00016	2·0
4.	0·20	0·054	0·007	0·00021	3·0
5.	0·08	0·022	0·007	0·000085	1·2
6.	0·10	0·027	0·008	0·0001	1·3
7.	0·15	0·041	0·01	0·00016	1·6
8.	0·25	0·068	0·005	0·00026	5·2
9.	0·15	0·041	0·003	0·00016	5·3
10.	0·15	0·041	0·02	0·00016	0·8
11.	0·10	0·027	0·007	0·0001	1·4
12.	0·015	0·0041	0·003	0·00001	0·33
13.	0·04	0·011	0·003	0·000042	1·4
14.	0·08	0·022	0·008	0·000085	1·1

In most of the above specimens the proportion of radiogenic strontium is 1–5 %: although not very appreciable, these proportions are nevertheless very significant. Had these Caledonian rocks been ancient

e.g. 1500×10^6 years), then the proportion of radiogenic strontium would have been as much as 20–30 % in some of the specimens.

In pegmatites complete data (% Rb, % total Sr, and age) on muscovite and biotite are very meagre, but one may infer that because pegmatitic muscovites invariably contain only small traces of strontium (frequently 0·001–0·01 %) and often contain appreciable traces of rubidium, the proportion of radiogenic strontium will frequently be considerable. In two ancient specimens of pegmatitic muscovite (Usakos, South-West Africa, and Game Reserve, eastern Transvaal) which were found to contain respectively 0·14 % Rb, 0·0005 % Sr, and 0·28 % Rb, 0·0012 % Sr, the proportions of radiogenic strontium have been calculated as 90 % and 70 % respectively, on the assumption that the ages of these minerals are about 1000×10^6 years. These high proportions of radiogenic strontium can by no means be regarded as being representative, and undoubtedly in many pegmatitic muscovites, in particular young ones poor in rubidia, the proportion of radiogenic strontium must be very much smaller. Thus Bray (17) analysed three specimens of pegmatitic muscovite from pre-Cambrian rocks from Colorado (see table 6) and found the mean strontium content to be 0·007 %. If we assume about 0·1–0·2 % Rb to be present (an amount frequently found in muscovite) and the ages of these pegmatites to be roughly 1000×10^6 years (Holmes, 18), about 0·0003–0·0006 % radiogenic strontium will be present and the proportion of radiogenic strontium will be approximately 5–10 %.

Noll (19) has also analysed strontium from pegmatitic muscovite and found only 0·001 % SrO: because this amount of strontium is very small one must conclude that much of it is radiogenic. A very small quantity of strontium (0·0035 %) was also found by Bray (17) in biotite from pegmatite associated with the Silver Plume granite of Colorado. Here again the proportion of radiogenic strontium must be very appreciable. In some other pegmatitic biotite specimens analysed by Bray much more strontium was found and very probably the proportion of radiogenic strontium is consequently much less.

Phlogopite.—Work carried out by the author (unpublished results) on a specimen of phlogopite from the Palabora complex, Transvaal, containing about 0·09 % Rb, showed that a very small quantity of strontium (0·0005–0·00008 %) was present and that a large proportion of the strontium is probably radiogenic.

Noll (19) analysed phlogopite from Bamle, Norway, and found less than 0·001 % Sr: since all specimens of phlogopite appear to contain

appreciable traces of rubidium, one may conclude that in the Bamle specimen an appreciable proportion of the strontium must be radiogenic.

Potash-felspar other than amazonite.—Several authors (e.g. Noll, 19) have shown that strontium tends to be considerably more abundant in felspar than in mica. This may be shown conclusively by separating both felspar and mica from the same rock. Thus Bray (17) separated potash-felspar and muscovite from granites and associated pegmatites, and found the following strontium contents (table 6).

TABLE 6. Content of Sr in felspar and mica from granites, Colorado.

No.	Description.	% SrO Potash-felspar.	% SrO Muscovite.	Ratio: % SrO (mica). % SrO (felspar).
1. Boulder Creek granite	Parent-rock ...	0·087	0·063	0·72
	Pegmatite ...	0·044	0·0055	0·12
2. Overland Mt. granite	Parent-rock ...	0·13	0·0098	0·075
	Pegmatite ...	0·13	0·009	0·07
3. Silver Plume granite	Parent-rock ...	0·081	0·015	0·18
	Pegmatite ...	0·061	0·0066	0·11

With the exception of the parent-rock felspar and muscovite from the Boulder Creek granite where the decrease of strontium in the muscovite relative to the felspar is not very marked, all the above muscovite specimens contain very much less strontium than the associated felspar. (Approximate ratio of % SrO in muscovite : % SrO in felspar = 1/10.) There is very little doubt that in the above specimens of felspar the proportion of radiogenic strontium is very low and usually less than 1 % of the total strontium.

Nockolds and Mitchell (16) also found an enrichment of strontium in potash-felspar relative to mica (biotite) in the Caledonian rocks they examined. The strontium contents of potash-felspars, together with other data on rubidium and radiogenic strontium, are given in table 7, where the specimen numbers correspond to the numbers assigned to the associated micas in table 5.

In each of these specimens of potash-felspar (with the exception of the aplite specimen) the concentration of total strontium is much greater than in the associated micas (table 5); the ratio % SrO in mica : % SrO in felspar varies from 1/10 to 1/50 (average 1/25).

Because of this marked increase in the amount of strontium in felspar compared with associated mica, the proportion of radiogenic strontium becomes extremely small and more or less negligible. Even if these rocks had been ancient, the proportion of radiogenic strontium would still be

Table 7. Amount of Rb and Sr in Scottish potash-felspars.

No.	% Rb.	% Rb^{87}.	% total Sr.	% radiogenic Sr.	Approx. prop. radiogenic Sr.
1.	0·04	0·011	0·2	0·000042	0·021 %
2.	0·04	0·011	0·1	0·000042	0·042
3.	0·06	0·016	0·2	0·000064	0·03
4.	0·04	0·011	0·2	0·000042	0·021
5.	0·2	0·054	0·005	0·00021	4·0*
6.	0·006	0·0016	0·2	0·0000064	0·003
7.	0·012	0·0032	0·2	0·000012	0·006
8.	0·06	0·016	0·1	0·000064	0·064
9.	0·06	0·016	0·1	0·000064	0·064
10.	0·04	0·011	0·2	0·000042	0·021
11.	0·06	0·016	0·08	0·000064	0·08
12.	0·02	0·0054	0·15	0·000021	0·021
13.	0·02	0·0054	0·1	0·000021	0·021
14.	0·08	0·021	0·2	0·000085	0·042

* Aplite.

insignificant. As already stated, the proportion of radiogenic strontium in the biotite specimens from these Caledonian rocks varies approximately from 1 to 5 %, whereas in the associated felspars (with the exception of the specimen of aplite) the proportion varies from 0·003 to 0·08 %, and thus the proportion of radiogenic strontium in the micas is about one hundred times greater than in felspar.

Mention has been made of the relative richness of rubidium in *hydrothermal* microcline from Varuträsk, Sweden, and since the phase of formation of this mineral is late, one should expect the amount of magmatic strontium to be very small, and hence the proportion of radiogenic strontium to be high. Hahn (3) mentions a mass spectrographic examination of strontium in a specimen of Varuträsk microcline which showed a very high proportion of radiogenic strontium. In this respect it is likely that ordinary hydrothermal microcline and amazonite are very similar; both are late hydrothermal and both contain appreciable amounts of rubidium and, probably in most cases, a high proportion of radiogenic strontium.

In potash-felspars other than the above two types the proportion of radiogenic strontium will probably almost always be very low. In plagioclases the proportion of radiogenic strontium will invariably be negligible.

Relative proportion of radiogenic strontium in rocks.

Amongst rocks, only in granites and similar types relatively rich in potash and hence also in rubidium, is the proportion of radiogenic

strontium in the total strontium sometimes likely to be appreciable. In more basic types of rocks magmatic strontium may increase considerably, particularly where much calcium is present, whereas the abundance of rubidium decreases sharply, and one may conclude therefore that even in the most ancient of the more basic rock varieties the proportion of radiogenic strontium will be negligibly small and of no significance.

Since the amount of total strontium varies very considerably in granites from different localities (about 0·001–0·3 % Sr) and because the amount of rubidium also tends to vary quite considerably (about 0·01–0·2 % Rb), the proportions of radiogenic strontium in various granites of like age will be very erratic. Hence it is more or less meaningless to assign an average strontium and rubidium value for granites and then calculate the proportion of radiogenic strontium in 'average granite' of different ages: more instructive information can be obtained by making calculations on the available data (although still meagre) for rubidium and strontium in granites and similar types, the ages of which are known approximately.

Caledonian rocks from Britain.—Reference has already been made to the rubidium and strontium contents of felspar and mica from Caledonian igneous rocks from Great Britain. In the rocks as a whole the proportion of radiogenic strontium is very small and more or less negligible.

Rapakivi-granite from Finland.—The analyses of several rapakivi-granites have been given by Sahama (20). For the calculation on the amounts of radiogenic strontium formed, an age of about 900×10^6 years has been used, and in this respect I was fortunate in being able to consult Dr. Kalervo Rankama, of the University of Helsinki, about the ages of several Finnish formations referred to in the text.

The data given in table 8 refer to Sahama's standard mixture of rapakivi-granites from eastern Fennoscandia and also to three specimens from the Salmi area.

TABLE 8. Amounts of Rb and Sr in granites, Finland.

Description.	% Rb.	% Rb^{87}.	% total Sr.	% radiogenic Sr.	Approx. prop. radiogenic Sr.
Standard mixture	0·15	0·04	0·009	0·0004	4·5%
Granite-porphyry boulder, Uomaa	0·10	0·027	0·0045	0·00027	6·0
Even-grained rapakivi-granite, 2 km. NW. of Koirinoja ...	0·09	0·025	<0·003	0·00025	<9·0
Ovoidic type, Pensanoja ...	0·11	0·03	0·007	0·0003	4·0

Sahama has also analysed some rapakivi-granites and mica-schist from Ihovaara hill, Suistamo, where these two formations are in contact. Analytical data for rapakivi-granite, mica-gneiss and also a mica-gneiss fragment in rapakivi-granite, and a contaminated specimen of rapakivi-granite, are given below (table 9). The age of the mica-gneiss has been taken to be about 1500×10^6 years.

TABLE 9. Amounts of Rb and Sr in granite and gneiss, Finland.

Description.	% Rb.	% Rb^{87}.	% total Sr.	% radiogenic Sr.	Approx. prop. radiogenic Sr.
Mica-gneiss, 1 km. E. of Ihovaara hill	0·07	0·018	0·035	0·00028	0·8%
Mica-gneiss from immediate vicinity of contact	0·06	0·016	0·027	0·00026	1·0
Mica-gneiss fragment in rapakivi-granite from contact ...	0·12	0·032	0·015	0·00052	3·4
Contaminated rapakivi-granite	0·16	0·044	0·006	0·00044	7·5
'Normal' rapakivi-granite ...	0·11	0·03	0·0035	0·0003	9·0

From these available analyses it seems that the proportion of radiogenic strontium in the rapakivi-granite is roughly constant (averages about 6–7 %) and the granite appears to contain a characteristically higher proportion of radiogenic strontium than the more ancient gneiss (average of two analyses 0·9 %).

Rocks from southern Finnish-Lapland.—Sahama (21) has published some interesting quantitative data on the abundance of the minor constituents in rocks from south Finnish-Lapland. All his specimens, several of which were granite types, were analysed for rubidium and strontium and since the approximate ages of several of the different formations may be assessed, the proportions of radiogenic strontium may be calculated in some instances. All the analyses for rubidium and strontium (total) in the Finnish rocks referred to in the next four tables have been taken from Sahama's paper.

(1) The ancient sedimentary gneisses of the Tuntsa-Savukoski-formation.—This formation is one of the most ancient in Scandinavia and although its age is not known accurately, it is probably about $1500–2000 \times 10^6$ years. Analytical data are given in table 10.

In each of these three specimens of ancient gneiss the proportion of radiogenic strontium is quite considerable (about 20 %).

(2) Ancient gneissic granites.—Analytical data on these rocks are given in table 11: an age of about 1500×10^6 years has been used for calculating the amounts of radiogenic strontium generated.

TABLE 10.

Description.	% Rb.	% Rb^{87}.	% total Sr.	% radiogenic Sr.	Approx. prop. radiogenic Sr.
Kyanite-mica-gneiss: Karhutunturi	0·08	0·022	0·0027	0·00048	20 %
Coarse mica-gneiss: Lyöpäköngäs	0·04	0·011	0·0009	0·00024	27
Gneiss: Ulmapaljakko	0·06	0·016	0·0027	0·00035	13

TABLE 11.

Description.	% Rb.	% Rb^{87}.	% total Sr.	% radiogenic Sr.	Approx. prop. radiogenic Sr.
Granite-gneiss: Pomovaaran ...	0·10	0·027	0·0027	0·00046	17 %
Granite-gneiss: Sarakkavaara	0·19	0·052	0·0027	0·00089	33
Granite-gneiss: western Sotatunturi ...	0·19	0·052	0·0054	0·00089	17
Granodiorite-gneiss: Kemijoen	0·03	0·008	0·027	0·00014	0·5
Granodiorite-gneiss: Värriöjoki	0·06	0·016	0·027	0·00027	1·0

Although a large number of specimens have not been analysed, it seems very probable that the granite types contain an appreciably higher proportion of radiogenic strontium (17–33 %) than the granodioritic types (0·5–1·0 %). This is only to be expected when one examines the abundance of some of the major constituents in the granite and granodiorite: the granite contains about three times more potash than the granodiorite, whereas the latter rock contains about three times as much calcium as the former. As is now well known, rubidium tends to be associated with potassium, whereas strontium tends to follow calcium in minerals.

(3) Hetta type of granite.—An age of about 1200×10^6 years for this granite has been assumed for calculating the data on radiogenic strontium given below in table 12.

TABLE 12.

Description.	% Rb.	% Rb^{87}.	% total Sr.	% radiogenic Sr.	Approx. prop. radiogenic Sr.
Granodiorite: Suasjärvi ...	0·05	0·014	0·09	0·00018	0·2 %
Gneissic granite: Piernakkaselkä	0·06	0·016	0·09	0·00021	0·2
Granite: Urakkaselkä	0·19	0·051	0·018	0·00065	3·5

In the granodiorite and gneissic granite a small proportion of the total strontium is radiogenic, whereas in the specimen of granite, the proportion of radiogenic strontium is about twenty times higher.

(4) Younger granites.—For calculating the data on radiogenic

strontium, given below in table 13, an age of about 900×10^6 years has been assumed for these granites.

TABLE 13.

Description.	% Rb.	% Rb^{87}.	% total Sr.	% radiogenic Sr.	Approx. prop. radiogenic Sr.
Granite: Untosenjärvi lake ...	0·19	0·051	0·018	0·0005	2·8 %
Granite: Korkeamaa	0·19	0·051	0·0027	0·0005	19
Granite: Eskelinen	0·10	0·027	0·018	0·00027	1·5
Coarse granite: Polvirova ...	0·10	0·027	0·0027	0·00027	10

The proportion of radiogenic strontium in these specimens varies considerably: in two of them the proportion is high, whereas in the other two specimens the proportion is appreciably lower, although by no means unusually low for granites.

In Sahama's paper the strontium and rubidium contents of various other rock types from south Finnish-Lapland are also given: in some of the rocks the proportion of radiogenic strontium is undoubtedly negligible (<0·001 % of total strontium), for example, in various basic rocks and also limestones, whereas in some formations the proportion of radiogenic strontium is very considerable. For example, strontium could not be detected in certain specimens of quartzite and should therefore be present in a concentration of less than 0·001 %; these quartzites contain on an average 0·05 % rubidium and assuming an approximate age of 1000×10^6 years, at least 15 % of the strontium is radiogenic.

Grängesberg iron-ore deposits, Sweden.—Landergren (22) has analysed several materials associated with the Grängesberg iron ores, and since his analyses include strontium and rubidium it is possible to calculate data on radiogenic strontium: an approximate age of 2000×10^6 years has been used for these calculations. Analytical data are given in table 14; the specimen numbers refer to Landergren's specimen numbers given in table 3 of his paper. Reference should be made to his paper for a more detailed account of the types of materials he analysed.

TABLE 14.

No.	% Rb.	% Rb^{87}.	% total Sr.	% radiogenic Sr.	Approx. prop. radiogenic Sr.
2	—	—	0·02	—	—
3	0·3	0·08	0·004	0·0018	45 %
4	<0·0003	<0·00008	0·01	<0·0000018	<0·018
5	0·02	0·0054	0·03	0·00012	0·4
6	0·09	0·024	0·02	0·00053	2·1
7	0·3	0·08	0·01	0·0018	18
8	0·1	0·027	0·001	0·0006	60

(*Table 14 continued*)

No.	% Rb.	$\%Rb^{87}$.	% total Sr.	% radiogenic Sr.	Approx. prop. radiogenic Sr.
9	—	—	0·002	—	—
10	0·04	0·011	0·002	0·00024	12 %
11	—	—	0·005	—	—
12	0·0003	0·00008	0·002	0·0000018	0·1
13	0·0003	0·00008	0·004	0·0000018	0·05
14	0·1	0·027	0·004	0·0006	15
15	0·4	0·11	0·007	0·0024	35
16	0·2	0·054	0·01	0·0012	12
17	—	—	0·02	—	—
18	—	—	0·02	—	—
19	0·0009	0·00024	0·02	0·0000053	0·025
20	0·5	0·14	0·006	0·0031	52
21	0·3	0·08	0·01	0·0018	18
22	0·0009	0·00024	0·004	0·0000053	0·13
23	—	—	0·01	—	—
24	0·2	0·054	0·01	0·0012	12
25	0·009	0·0024	0·003	0·000053	1·8
26	<0·0003	<0·00008	0·0003	<0·0000018	<0·5
28	0·08	0·022	0·001	0·00048	48
29	0·009	0·0024	<0·0003	0·000053	>18
30	0·0009	0·00024	0·008	0·0000053	0·6
31	<0·0003	<0·00008	<0·0003	<0·0000018	—
32	—	—	<0·0003	—	—
33	<0·0003	<0·00008	<0·0003	<0·0000018	—
34	0·005	0·0014	0·001	0·00006	6·0
35	—	—	<0·002	—	—
36	—	—	0·003	—	—
39	0·006	0·0016	0·009	0·000035	0·6
40	—	—	0·0003	—	—
41	—	—	0·0007	—	—
42	0·14	0·038	0·001	0·00084	84
43	0·0009	0·00024	<0·0003	0·0000053	>1·8
44	—	—	<0·0003	—	—
45	—	—	<0·0003	—	—
46	—	—	0·0008	—	—
47	0·08	0·022	0·005	0·00048	9·6
48	0·004	0·0011	0·003	0·000024	0·8
49	0·2	0·054	0·001	0·0012	100
50	<0·0003	<0·00008	0·003	<0·0000018	<0·06
51	0·003	0·0008	0·002	0·000018	0·9
52	0·03	0·008	0·02	0·00018	0·9
53	0·009	0·0024	0·006	0·000053	0·9
54	0·04	0·011	0·001	0·00024	24 %
55	<0·0003	<0·00008	0·01	<0·0000018	<0·018
56	0·0009	0·00024	0·02	0·00000053	0·025
57	<0·0003	<0·00008	0·02	<0·0000018	<0·009
58	0·005	0·0014	0·03	0·00006	0·2
59	0·0009	0·00024	<0·0003	0·0000053	>1·8
60	0·25	0·068	<0·0003	0·0015	>100

Reference to the above table shows that the proportion of radiogenic strontium in the total strontium is extremely erratic and varies from negligible proportions to about 100 % radiogenic strontium. In this respect the above collection of minerals is indeed interesting and provides one with a good indication of how the proportion of radiogenic strontium varies from specimen to specimen: unfortunately for our purpose the author has not provided detailed descriptions of the minerals analysed.

The Ca–Sr–Ba association in minerals.

The association of these three alkaline earths in minerals and rocks is frequently discussed by geologists; in particular Ca/Sr and Ba/Sr ratios in different minerals and rocks has elicited considerable interest. In these discussions all strontium is assumed to be magmatic, but because the proportion of radiogenic strontium may on occasion be appreciable and in a few instances may predominate, cognizance should therefore be taken of the rubidium content and age of each specimen in these discussions.

References.

1. Hahn (O.) and Walling (E.), Zeits. Anorg. Allgem. Chem., 1938, vol. 78, p. 236. [M.A. **8**–156.]
2. Hemmendinger (A.) and Smythe (W. R.), Physical Rev., 1937, vol. 51, p. 1052.
3. Hahn (O.), Geol. För. Förh. Stockholm, 1944, vol. 66, p. 90.
4. Goldschmidt (V. M.), Skrift. Norske Vidensk. Akad., Math.-Nat. Kl., 1938 (for 1937), no. 4, p. 29. [M.A. **7**–166.]
5. Noddack (I. and W.), Angew. Chem., 1936, vol. 49, p. 1. [M.A. **6**–205.]
6. Ahrens (L. H.), Amer. Min., 1947, vol. 32, p. 44. [M.A. **10**–113.]
7. Goldschmidt (V. M.), Bauer (H.), and Witte (H.), Nachr. Gesell. Wiss. Göttingen, Math.-Phys. Kl., Sect. IV, 1934, vol. 1, no. 4, p. 39.
8. Ahrens (L. H.), Trans. Geol. Soc. South Africa. (In the press.)
9. Strassmann (F.) and Walling (E.), Ber. Deutsch. Chem. Gesell., Abt. B, 1938, vol. 71, p. 1. [M.A. **7**–498.]
10. Tolmachev (Y. M.) and Filippov (A. N.), Compt. Rend. Acad. Sci. URSS, 1935, vol. 1, p. 323. [M.A. **6**–377.]
11. Ahrens (L. H.), Trans. Geol. Soc. South Africa, 1946, vol. 48 (for 1945), p. 207.
12. Adamson (O. J.), Geol. För. Förh. Stockholm, 1942, vol. 64, p. 19. [M.A. **8**–353.]
13. Heyden (M.) and Kopfermann (H.), Physikal. Zeits., 1937, vol. 38, p. 960.
14. Brewer (A. K.), Journ. Amer. Chem. Soc., 1938, vol. 60, p. 691.
15. Oftedal (I.), Norsk Geol. Tidsskr., 1943, vol. 22 (for 1942), p. 1. [M.A. **9**–278.]
16. Nockolds (S. R.) and Mitchell (R. L.), Trans. Roy. Soc. Edinburgh, 1948, vol. 61, p. 533.
17. Bray (J. M.), Bull. Geol. Soc. Amer., 1942, vol. 53, p. 765. [M.A. **8**–324.]
18. Holmes (A.), The age of the earth. London, 1937, p. 204. [M.A. **7**–8.]

19. Noll (W.), Chem. d. Erde, 1934, vol. 8, p. 507. [M.A. **6**–87.]
20. Sahama (T. G.), Compt. Rend. Soc. Géol. Finlande, 1945, no. 18, p. 16. [M.A. **9**–277.]
21. Sahama (T. G.), Bull. Comm. Géol. Finlande, 1945, no. 135. [M.A. **9**–308.]
22. Landergren (S.), Ing.-Vet.-Akad. Handlingar, Stockholm, 1943, no. 172. [M.A. **10**–219.]

An improved polarizing microscope. III. The slotted ocular and the slotted objective.[1]

By A. F. Hallimond, M.A., Sc.D., F.G.S.
Museum of Practical Geology, London, and
E. Wilfred Taylor, C.B.E., F.R.M.S., F.Inst.P.
Messrs. Cooke, Troughton & Simms, Ltd., York.

[Read November 6, 1947.]

I. *Introduction.*

MEASUREMENTS with the petrological microscope may be divided into those made with the orthoscopic and those with the conoscopic arrangements. It was early realized that if the micrometer scale or compensator was inserted in the focal plane of the ocular, the same apparatus would serve for measurements of both kinds, provided that a Bertrand lens was available. The method was described by A. B. Dick[2] as early as 1888 in a form of microscope which has remained popular with many workers up to the present time. Additional slots at the level of the focal plane of the ocular were cut through the mount and the upper part of the microscope tube. Most European manufacturers, however, continued to provide only the usual slots in the lower part of the tube. These are often the sole means of inserting compensators, which in many cases cannot be focused at all by the eyepiece, even with the help of a slide for the Bertrand lens. The quartz-wedge cannot then be used, and recourse must be had to compensators of Nikitin type, such as those of Berek[3] and Ehringhaus.[4] To meet this difficulty, F. E. Wright[5] devised a well-known special ocular, resembling that described by J. Amann,[6] which serves to convert the standard type of tube to a form substantially similar to that used in Dick's microscope. An inevitable defect is that, since the eyepiece is to be placed in the unslotted tube, the slots must stand at a level above the top of the tube, with the

[1] Published by permission of the Director, Geological Survey and Museum.
[2] A. B. Dick, Min. Mag., 1888, vol. 8, pp. 160–163.
[3] M. Berek, Zentralbl. Min., 1913, pp. 388, 427, 464, 580.
[4] A. Ehringhaus, Zeits. Krist., 1931, vol. 76, pp. 315–321. [M.A. 5–127.]
[5] F. E. Wright, Amer. Journ. Sci., 1910, ser. 4, vol. 29, pp. 415–417.
[6] J. Amann, Zeits. wiss. Mikroskop., 1894, vol. 11, p. 440.

result that the tube-length is increased and a special Bertrand lens may be required.

All these slotted oculars required a cap nicol, and their use has been restricted, no doubt owing to the resulting limitations of field and eye-distance. With the introduction of polarizing film, it has become possible to design an ocular having an internal analyser of the usual sliding type, so that these inconveniences can be eliminated, though there might still remain the defect of an increased tube-length. In the ocular here described both difficulties have been fully met, since it is adapted to microscopes (Cooke Research and Universal models) in which the upper part of the tube can be replaced by a special ocular tube having slots at the correct level.

The second accessory to be described below is the slotted objective, a simpler device which renders possible the direct use of a graduated quartz-wedge over the interference-figure, but not over the orthoscopic image. The range of utility might at first seem to be severely restricted in comparison with the slotted ocular, but this is not the case, for it can be shown that measurements of extinction and birefringence may be made with greater accuracy on the interference-figure than on the orthoscopic image. Conoscopic methods are, in fact, to be preferred even when a slotted ocular is available, the principal advantages of the latter being in ease of manipulation, greater magnification, and the possibility of inserting micrometers over the orthoscopic image. For use with the universal stage it is possible to obtain a one-inch objective with slots, but most objectives will require compensators in the tube or eye-piece, in which case the quartz-wedge must be used in a slotted ocular.

II. *A revised slotted ocular.*

The general arrangement (fig. 1) resembles that already familiar to users of the Dick and Wright eyepieces. The new polaroid analyser and compensating glass disk are carried in a sliding fitting *A* immediately below the positive eyepiece *B*. The ocular itself[1] is a modified form of Kellner eyepiece (×10) which is very comfortable to use, and is characterized by freedom from distortion and an unusual eye-clearance; an important feature, not always to be found in ordinary wide-angle eye-pieces, is that owing to the great width of the eye-lens the whole field is visible even when the eye is at the correct and rather distant eyepoint. It is carried in a sliding tube with a locking ring *C*, which permits the

[1] E. W. Taylor, The inverting eyepiece and its evolution. Journ. Sci. Instruments, 1945, vol. 22, p. 43, especially fig. 10 and para. 10.

focus to be adjusted on the quartz-wedge or cross-lines as required. The wedge and other compensators and micrometer scales can be inserted in carriers *D* fitting the slots, which are wide enough to accommodate micrometer nets, &c. that cover the whole field. An iris diaphragm *E* which is sufficiently defined though not sharply in focus can be used to isolate a mineral grain in the centre of the field. A brilliant small interference-figure due to the grain can then be examined in the Ramsden

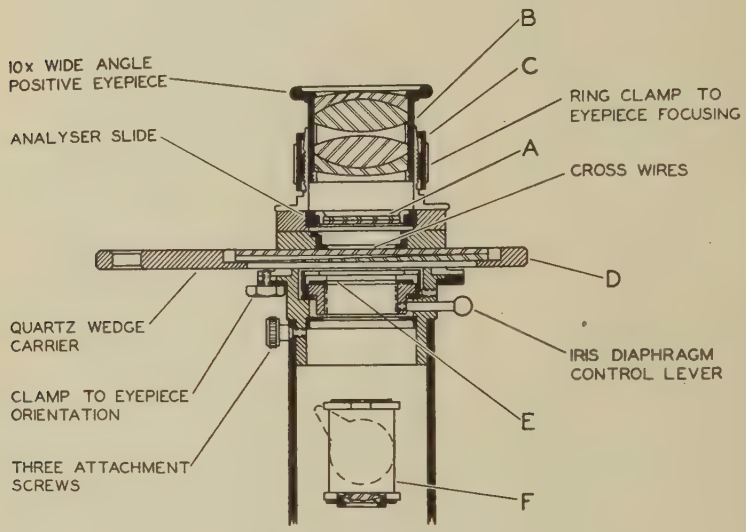

FIG. 1. Improved slotted ocular (in section). Half actual size.

circle by means of a $\times 10$ hand-lens (Becke or Klein method). It is possible, however, to obtain a similar degree of selectivity by bringing in the ordinary Bertrand lens *F* with its selecting diaphragm, in which case the figure is seen at greater magnification.

The ocular is fitted by removing the ordinary eye-tube at the shoulder above the Bertrand fitting and attaching the keyed special tube of the slotted ocular. The focal plane of the latter is then at the normal level for use with the Bertrand lens.

Accessories.—The equipment for all ordinary determinative work may be restricted to the following:

Graduated quartz-wedge; $\frac{1}{4}$ and 1λ compensator plates, preferably in rotatable mounts; Nakamura half-shadow plate (biquartz) if great accuracy is desired in setting extinction; net and other micrometers. It is advantageous if the wedge and compensators are of standard size

so that they can be used in the tube or objective slots of the microscope; special carriers being provided by which they can be inserted in the slotted ocular when desired.

III. *The slotted objective.*

This device was introduced some years ago in metallurgical microscopes made by Messrs. Cooke, Troughton & Simms. When combined with the quartz-wedge it offers a very simple and yet highly accurate means for making the usual determinations on crystal sections. Slots of standard dimensions, equal to those in the microscope tube, are provided in the tubular portion of the objective mount above the lenses, a construction which is normally practicable for one-inch and higher powers. A graduated quartz-wedge can then be inserted almost in the same plane as the interference-figure and read by means of the Bertrand lens, any slight difference in focus being corrected by adjusting the eye-lens of the eyepiece. Other compensators or opaque stops can be used if desired. In fig. 2 the slotted 1/6th objective is shown in plan and section with a quartz-wedge *A* in position.

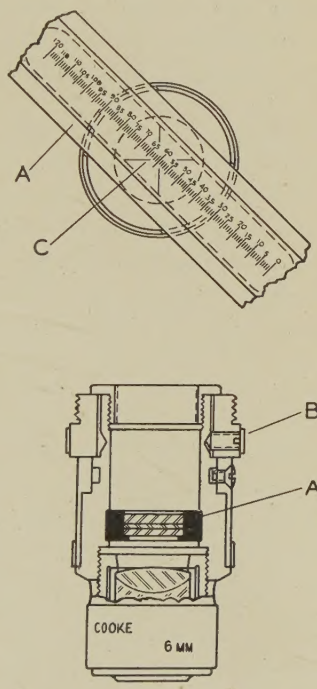

FIG. 2. Slotted objective with central part of a quartz-wedge in position (in part plan and section). Actual size.

Orientation.—The slots must be at the 45° position. The objective is screwed firmly into the objective holder and the small set-screws *B* near the top of the mount are released. The slotted part is then rotated with the quartz-wedge in place until the diagonal markings *C* provided near the centre of the wedge are parallel with the cross-lines in the eyepiece, at which position the set-screws should be locked.

The equipment will be the same as for the slotted ocular, but without the micrometers and special carriers. If the black zero band is to be obtained by inserting a first-order compensator in the tube slots, the objective (like the slotted ocular) must be oriented so that the

quartz-wedge compensates the first-order plate. The results are then comparable with those obtainable by means of the Wright compensated wedge. If the slotted objective is used with a sprung objective changer, care should be taken not to disturb the centring during manipulation of the compensators.

Note on conoscopic methods (A. F. H.).

The following note, in which attention is drawn to the advantage of adjusting both extinction and compensation by means of the interference-figure, applies generally both to the slotted ocular and the slotted objective.

Path-difference.—It has been customary to measure the path-difference by compensating the interference effect in the orthoscopic image of the desired mineral grain, which must be placed at the centre of the field. Under these conditions it is often very instructive to note the appearance of the interference-figure on introducing the Bertrand lens.[1] The light coming from the interference-figure is, of course, all utilized in forming the orthoscopic image, and in many cases, especially with objectives of high power, it is at once evident that a great deal of uncompensated light is present. Compensation is, in fact, confined to one of the lemniscates (or another curve if the compensator is not 'homogeneous', e.g. a quartz-wedge), which now appears as a dark curve bordered by the usual sequence of bands. There is sometimes so much uncompensated light present that the darkening is hardly appreciable in the orthoscopic image. It is usual, therefore, to eliminate the oblique rays as much as possible by closing the condenser iris. This leads to a sharper compensation but unfortunately the orthoscopic image is then much impaired by excessive relief due to the narrow aperture, and by the weakness of the illumination. A great improvement in accuracy can be obtained if compensation is adjusted on the interference-figure (conoscopic method)[2] instead of the orthoscopic image. On closing the condenser iris the brightness of the central area is not diminished, and there

[1] F. Rinne and M. Berek, Anleitung zu optischen Untersuchungen mit dem Polarisationsmikroskop, 1934, p. 124.

[2] Such methods were referred to as 'stauroscopic' in an earlier paper (Min. Mag., 1946, vol. 27, pp. 183–5). The original implication of this term seems rather obscure. It first appears in reference to the 'stauroscope' of von Kobell, by which extinction was adjusted with the aid of the interference-figure due to a calcite plate. It was later used, but rarely, as a general term for any methods of determining the extinction position (H. Rosenbusch, Mikroskop. Physiogr., 5th edit. by E. A. Wülfing, 1921, vol. 1, pt. 1, p. 435). 'Conoscopic' seems free from objection and will be employed instead.

is no direct effect from the relief, since the surface is not in focus. The darkest point in the compensated lemniscate can now be adjusted to coincide very closely with the centre of the interference-figure; i.e., compensation is being made precisely for the ray normal to the crystal section, and the field is limited by the Bertrand diaphragm.

If a quartz-wedge is being used, it is convenient to set the compensation band (which in the conoscopic method is not necessarily perpendicular to the sides of the wedge) on the cross-lines of the eyepiece and then open the condenser iris or remove the Bertrand lens so that the graduations are visible against a wider field. Finally, a zero reading is taken after the object has been removed, and the path-difference is read from a calibration scale obtained by reading the interference-bands for the light used, with crossed and parallel positions of the analyser. On account of the dispersion of the birefringence the wedge should strictly be calibrated for the wave-length to be used. It is not quite accurate to assume that the path-difference is in the same ratio to the reading for all colours, though the error is small. For an ordinary quartz-wedge the zero band is missing since it coincides with the ultimate thin end of the wedge. Wright and others have devised combination wedges having a parallel crystal plate mounted under the wedge to compensate, say, the first-order interference-band, which then becomes the zero band and is easily read. The same result is obtained very simply, if additional slots are available, by inserting an ordinary first-order compensating plate in the tube slots: the zero band then appears at the desired position on the quartz-wedge.[1]

The graduated quartz-wedge can be read easily to one-twentieth of one wave-length, which is sufficient for an accuracy of 0·001 in the birefringence of a rock section. Its range can be extended by replacing the gypsum-plate in the second slots by a thick compensator of known additional path-difference, say, one order less than the wedge itself, so that the value can be checked by compensating it against the wedge.

Over a uniform field the distribution of intensity in the compensation band of a quartz-wedge is symmetrical, and the true compensation position is therefore the centre of the band. If the crystal section varies rapidly and unsymmetrically in birefringence for directions on either side of the axial ray, there may be a slight error due to the tendency to set the middle of the band, but in practice this is negligible and in any case the readings are nearly always taken on a principal optical direction, which is symmetrical.

[1] J. Amann, loc. cit.

If a 'homogeneous' compensator is used (e.g. Soleil), accurate setting may be improved by using a biquartz-plate, but with a quartz-wedge the gradation of the wedge itself gives the equivalent of a photometric setting for the centre of the dark band, which is quite narrowly defined if the illumination is sufficiently bright. J. Amann (loc. cit.) proposed to place the slit of a microspectroscope across the wedge like a cross-wire, and to adjust the wedge in white light so that the dark band in the spectrum indicated compensation at the desired wave-length; this does not seem to be more accurate than setting in monochromatic light. Compensators of the Nikitin type, while very convenient and compact, are probably somewhat less accurate than a well-made quartz-wedge. The latter has the great advantage of an almost linear scale, while that for some rotary compensators shows marked curvature between the half-wave values used in calibration, so that accurate interpolation can only be made with the help of the function calculated for the wedge.

Extinction.—As with path-difference, it is advisable to test the light used in the orthoscopic image by bringing in the Bertrand lens. The 'zero isogyre' is then seen and at the true extinction position it crosses the centre of the field. But there is then a proportion of light present from the rest of the interference-figure, and the first precaution is to exclude this by closing the condenser iris. In a bright light the centre of the isogyre can often be adjusted with sufficient accuracy by this means alone, but if the isogyre is broad the true extinction position may be detected by inserting a biquartz above the interference-figure. The advantages of increased brightness and the absence of irregularities in the field are the same here as in estimating path-difference.